2024-01

# Essential omega3 fatty acids are depleted in sea ice and pelagic algae of the Central Arctic Ocean

Schmidt, K

https://pearl.plymouth.ac.uk/handle/10026.1/21960

RESEARCH ARTICLE

Global Change Biology WILEY

# Essential omega-3 fatty acids are depleted in sea ice and pelagic algae of the Central Arctic Ocean

Katrin Schmidt[1] | Martin Graeve[2] | Clara J. M. Hoppe[2] | Sinhué Torres-Valdes[2] | Nahid Welteke[2] | Laura M. Whitmore[3] | Philipp Anhaus[2] | Angus Atkinson[4] | Simon T. Belt[1] | Tina Brenneis[2] | Robert G. Campbell[5] | Giulia Castellani[2] | Louise A. Copeman[6] | Hauke Flores[2] | Allison A. Fong[2] | Nicole Hildebrandt[2] | Doreen Kohlbach[7,8] | Jens M. Nielsen[9,10] | Christopher C. Parrish[11] | Cecilia Rad-Menéndez[12] | Sebastian D. Rokitta[2] | Sandra Tippenhauer[2] | Yanpei Zhuang[13]

[1]School of Geography, Earth and Environmental Sciences, University of Plymouth, Plymouth, UK

[2]Alfred-Wegener-Institut Helmholtz-Zentrum für Polar- und Meeresforschung, Bremerhaven, Germany

[3]International Arctic Research Center, University of Alaska Fairbanks, Fairbanks, Alaska, USA

[4]Plymouth Marine Laboratory, Plymouth, UK

[5]Graduate School of Oceanography, University of Rhode Island, Narragansett, Rhode Island, USA

[6]NOAA Alaska Fisheries Science Center, Hatfield Marine Science Center, Newport, Oregon, USA

[7]Norwegian Polar Institute, Fram Centre, Tromsø, Norway

[8]Department of Arctic and Marine Biology, The Arctic University of Tromsø, Tromsø, Norway

[9]Cooperative Institute for Climate, Ocean, and Ecosystem Studies, University of Washington, Seattle, Washington, USA

[10]NOAA Alaska Fisheries Science Center, Seattle, Washington, USA

[11]Department of Ocean Sciences, Memorial University of Newfoundland, St. John's, Newfoundland, Canada

[12]Culture Collection of Algae and Protozoa, Scottish Association for Marine Science, Oban, UK

[13]Polar and Marine Research Institute, Jimei University, Xiamen, China

**Correspondence**
Katrin Schmidt, School of Geography, Earth and Environmental Sciences, University of Plymouth, Plymouth, UK.
Email: katrin.schmidt@plymouth.ac.uk

**Funding information**
Bundesministerium für Bildung und Forschung, Grant/Award Number: 03F0804A, 03F0810A and 03F0916A; Directorate for STEM Education, Grant/Award Number: OPP-1735862; Natural Environment Research Council, Grant/Award Number: NE/R017050/1 and NE/S002502/1; Norges Forskningsråd, Grant/Award Number: RCN # 276730

## Abstract

Microalgae are the main source of the omega-3 fatty acids eicosapentaenoic acid (EPA) and docosahexaenoic acid (DHA), essential for the healthy development of most marine and terrestrial fauna including humans. Inverse correlations of algal EPA and DHA proportions (% of total fatty acids) with temperature have led to suggestions of a warming-induced decline in the global production of these biomolecules and an enhanced importance of high latitude organisms for their provision. The cold Arctic Ocean is a potential hotspot of EPA and DHA production, but consequences of global warming are unknown. Here, we combine a full-seasonal EPA and DHA dataset from the Central Arctic Ocean (CAO), with results from 13 previous field studies and 32 cultured algal strains to examine five potential climate change effects; ice algae loss, community shifts, increase in light, nutrients, and temperature. The algal EPA and

DHA proportions were lower in the ice-covered CAO than in warmer peripheral shelf seas, which indicates that the paradigm of an inverse correlation of EPA and DHA proportions with temperature may not hold in the Arctic. We found no systematic differences in the summed EPA and DHA proportions of sea ice versus pelagic algae, and in diatoms versus non-diatoms. Overall, the algal EPA and DHA proportions varied up to four-fold seasonally and 10-fold regionally, pointing to strong light and nutrient limitations in the CAO. Where these limitations ease in a warming Arctic, EPA and DHA proportions are likely to increase alongside increasing primary production, with nutritional benefits for a non-ice-associated food web.

## 1 | INTRODUCTION

Two vitamins, four minerals and two omega-3 fatty acids (FAs) are considered key when assessing the 'nutrient richness' of various food groups for human consumption (Golden et al., 2021). The two FAs are the long-chain polyunsaturated eicosapentaenoic acid [EPA, 20:5(*n*-3)] and docosahexaenoic acid [DHA, 22:6(*n*-3)], which benefit cell membrane function, neurological development, cognition, visual acuity, cardiovascular health, the immune system, and anti-inflammation among others (Calder, 2015; Rimm et al., 2018). Humans have a low efficiency for de novo synthesis of EPA and DHA from precursor FAs and rely on dietary uptake (Anderson & Ma, 2009). The same holds true for most heterotrophs, including zooplankton, fish and terrestrial consumers, which require EPA and DHA to aid their growth, reproduction and survival, but lack efficient synthesis (Jónasdóttir et al., 1995; Kainz et al., 2004; Litzow et al., 2006; Parrish, 2009). Consequently, aquatic and terrestrial food webs depend on micro- and macroalgae as primary producers of these 'essential' molecules, on trophic transfer for acquisition and on selective retention for long-term usage (Baird, 2022; Galloway et al., 2012; Gladyshev et al., 2009; Schmidt et al., 2012). However, a challenge for EPA and DHA provision to humans and other consumers comes from the highly variable FA composition of marine microalgae; internally set by their phylogeny and modified by external conditions (Galloway & Winder, 2015; Guschina & Harwood, 2009).

Temperature is considered a key driver of the EPA and DHA proportions in microalgae and other organisms due to their homeoviscous adaptation (Sinensky, 1974). This adaptation allows cell membranes to maintain a desired level of fluidity, and therefore function, under environmental conditions that would otherwise enhance or reduce their rigidity. There are several pathways to adjust membrane fluidity including a shift in the ratio of 'flexible' (unsaturated) versus 'inflexible' (saturated) FAs within the phospholipid bilayer (Parrish, 2013). Since EPA and DHA are more flexible than their saturated counterparts, their incorporation into membranes is reduced when temperatures rise (Fuschino et al., 2011; Rousch et al., 2003). Indeed, a data synthesis of >300 FA profiles from cultured marine and freshwater diatoms showed that decreasing EPA proportions within the algae

total fatty acid (TFA) pool coincides with higher temperatures (Hixson & Arts, 2016). The same study predicts that with a 2.5°C increase in water temperature, the global EPA and DHA production will drop by up to ~28%, with adverse effects for higher trophic levels (Hixson & Arts, 2016). While an algal strains' physiological response to rising temperatures might partly be mitigated through rapidly evolving thermal reaction norms of FA compositions (O'Donnell et al., 2019), a co-occurring increase in water column stratification and taxonomic shift from EPA- or DHA-producing eukaryotes to EPA- and DHA-deficient cyanobacteria might add to direct physiological effects of temperature rise (Schmidt et al., 2020).

Large compilations of FA profiles from epipelagic and deep-sea communities, broadly separated into three zones (polar, temperate, tropical), indicate that polar organisms contain, on average, greater EPA and DHA proportions than their warmer ocean counterparts (Colombo et al., 2017; Parzanini et al., 2019). In microalgae from Arctic sea ice and under-ice blooms, EPA proportions can be as high as 25%–30% of TFA (Duerksen et al., 2014; Wang et al., 2014), that is, more than twice the global average for marine microalgae (12% EPA: Colombo et al., 2017). However, Arctic sea ice studies have also shown two- to three-fold regional and seasonal differences in the EPA and DHA proportions of microalgae, despite a narrow temperature range (Budge et al., 2008; Leu et al., 2010; Wang et al., 2014). These differences have been attributed to the taxonomy of the bloom-forming microalgae, to a potential lack of nutrients, or detrimental effects of high irradiance (Leu et al., 2010, 2020; Wang et al., 2014).

All three of these factors may change with on-going loss of sea ice and faster Atlantic currents entering the Arctic (Ardyna & Arrigo, 2020).

In line with previous considerations (e.g., Jónasdóttir, 2019), we hypothesize that microalgal EPA and DHA proportions will decrease in a future Arctic due to a suite of proposed mechanisms: (1) Loss of sea ice leading to regional absence of ice algae blooms, known for their high content of polyunsaturated fatty acids (PUFA), such as EPA and DHA (Søreide et al., 2010); (2) reduced snow cover and sea ice thickness leading to increased irradiance in sea ice, which can have negative effects on the PUFA content of ice algae (Leu et al., 2010); (3) increased

freshening of Arctic surface waters enhancing stratification and therefore reducing vertical mixing of nutrients essential for algal EPA and DHA production (Guschina & Harwood, 2009); (4) non-diatoms that are deficient in EPA (Dalsgaard et al., 2003) taking over from diatoms as key primary producers in the Arctic (Jónasdóttir, 2019; Li et al., 2009); (5) higher temperatures reducing the algae requirements for EPA and DHA in a homeoviscous adaptation (Hixson & Arts, 2016).

To investigate these proposed mechanisms, we used a three-pronged approach that includes a new, full-seasonal dataset from the Central Arctic Ocean (CAO) acquired during the recent MOSAiC expedition (October 2019–October 2020), a meta-analysis of 13 previous field studies in Arctic shelf regions and the CAO (Table 1), and newly conducted laboratory experiments with 32 cold-water algal strains. Point 1, above, is covered by eight field studies, in either spring or summer, where sea ice and pelagic particulate organic matter (POM) were sampled simultaneously for FA analysis. Points 2 and 3 were investigated via the 'natural field experiment' of the Arctic, showing a strong seasonal cycle in photosynthetically active radiation (PAR) and strong regional differences in nutrient inventories (Castellani et al., 2022; Randelhoff et al., 2020) against a relatively constant temperature background of the ice-covered surface ocean. Further insights come from culture experiments with the keystone under-ice diatom species, *Melosira arctica*, explicitly addressing the effect of nutrient supply, light intensity or temperature on its EPA and DHA proportions. Point 4 was studied via 32 culture experiments including Arctic sea ice diatoms (e.g., *Nitzschia frigida, Attheya* spp.) as well as those non-diatom species that are becoming increasingly prominent in the Arctic, for example the coccolithophore *Emiliania huxleyi* (synonym *Gephyrocapsa huxleyi*) (Oziel et al., 2020), the prymnesiophyte *Phaeocystis pouchetii* (Assmy et al., 2017; Orkney et al., 2020), the chlorophyte *Micromonas* spp. (Li et al., 2009) and the cyanobacterium *Synechococcus* spp. (Paulsen et al., 2016). To address Point 5, the culture experiments were run at two different temperature-light combinations imitating 'colder' and 'warmer' summer conditions in the low-latitude Arctic.

Taken together, our multiple approaches do not support the hypothesized reduction of EPA and DHA under warmer and more ice-free Arctic conditions, but instead point to current limitations due to low light and/or nutrient availability. These control mechanisms imply the potential for EPA and DHA increases, rather than decreases, in those parts of the CAO where reductions in ice cover and enhanced atmospheric forcing lead to longer growing seasons and stronger vertical mixing of nutrients.

## 2 | MATERIALS AND METHODS

### 2.1 | Microalgae cultures and experiments with *M. arctica*

#### 2.1.1 | Microalgae cultures

In 2022, we conducted FA analysis on 32 cold-water strains that were isolated in the Arctic (25 strains), Southern Ocean (2 strains) or North Atlantic (5 strains), and included diatoms, chlorophytes, haptophytes, cryptophytes, chrysophytes, dinoflagellates and cyanobacteria (Table S1). These strains were either obtained from commercial culture collections (Culture Collection of Algae and Protozoa, CCAP, Oban, Scotland, and Roscoff Culture Collection, RCC, Roscoff, France) or provided by the Alfred-Wegener-Institute—Helmholtz-Centre for Polar and Marine Research, Bremerhaven, Germany (AWI). The cultures were inoculated in 50 mL Erlenmeyer conical flasks with 25 mL of F/2 medium and added 60 μmol L$^{-1}$ silicate for diatoms (Guillard & Ryther, 1962). The algae strains were grown for 4 weeks at low temperature (3–4°C), low light intensity (~10 μmol photons m$^{-2}$ s$^{-1}$) and a light: dark cycle of 12:12 h. The algae growth rates were not monitored, but with these culture conditions and time span, the strains usually reach late exponential-early stationary growth (C. Rad-Menéndez and I. Probert, personal communication). From each strain, two 5 mL technical replicates were filtered via a vacuum pump (−20 kPA) onto pre-combusted (12 h, 450°C) 25 mm Whatman GF/F filters, freeze dried and stored in aluminium foil at −20°C until FA analysis.

*Note*: Three of the strains from CCAP (CCAP-1023/3, CCAP-1029/29, CCAP-1029/30) were obtained and analyzed as '*Fragilariopsis* sp.' but subsequently identified as '*Grammonema* sp.'

#### 2.1.2 | Experiments with *M. arctica*

The experiments with *M. arctica* were carried out at the AWI in 2021 and 2022, using a strain that was isolated in the CAO in 2015 (79.56°N, 4.84°W; strain PS93.1_030). The strain was grown as semi-continuous batch cultures under six different environmental conditions including the species' natural range of temperature, light and nutrient availability (Fernández-Méndez et al., 2014; Spilling & Markager, 2008). Therefore, low temperatures (0–1°C) were combined with high and low light intensity (10 and 100 μmol photons m$^{-2}$ s$^{-2}$), each with high and low nutrient supply (details below), and higher temperatures (3 and 6°C) with high light and nutrient availability (Figure S1). Experiments were performed with four biological replicates in sterile 1-L Schott bottles in temperature-controlled rooms, with bottles at 3 and 6°C being immersed in water-filled aquaria for additional temperature stability. Day light lamps (Biolux T8, 6500K; Osram) provided continuous light and irradiance levels were adjusted with a black mesh fabric and measured using a 4π spherical sensor (Li-Cor) and data logger (ULM-500; Walz). Cells were cultivated in 0.2-μm sterile-filtered Arctic seawater (salinity 33.5), with or without added macronutrients, vitamins and trace metals according to F/2 or F/20 media (Guillard & Ryther, 1962). Initial nutrient concentrations in set-ups with F/20 media were 10.4 ± 0.24 μmol L$^{-1}$ nitrate-and-nitrite, 18.1 ± 1.36 μmol L$^{-1}$ silicate and 1.2 ± 0.19 μmol L$^{-1}$ phosphate. In set-ups without added medium, initial nutrient concentrations were 1.8 ± 0.07 μmol L$^{-1}$ nitrate-and-nitrite, 14.4 ± 2.3 μmol L$^{-1}$ silicate and 0.4 ± 0.01 μmol L$^{-1}$ phosphate. To minimize changes in carbonate chemistry and to remain close to natural population densities, cultures were diluted every 1–2 weeks

**TABLE 1** Overview of published studies that were sourced for EPA and DHA proportions in sea ice and/ or pelagic POM to compare with data from MOSAiC: Arctic region, primary productivity (PP), season, temperature, sampling information, data type and -source.

| Arctic region | PP | Lat | Lon | Season | $T_{min}$ (°C) | $T_{max}$ (°C) | No. profiles | Sampling device | Sampling layer/ depth (m) | FA unit | 16 FA (%) mean±SD | Associated study | Source |
|---|---|---|---|---|---|---|---|---|---|---|---|---|---|
| **Ice-POM** | | | | | | | | | | | | | |
| Bering Sea | | 60–63°N | 172–177°W | Apr–May 2009 | | | 8 | Ice corer | Bottom section | % | 91±5 | Wang et al. (2014) | B |
| | | 58–63°N | 169–175°W | Mar–May 2010 | | | 16 | Ice corer | Bottom section | % | 87±5 | Wang et al. (2014) | B |
| Barents Sea | | 81–82°N | 28–31°E | May 2021 | | | 10 | Slurp gun | Bottom section | % | 89±1 | Kohlbach et al. (2022) | C |
| | | 81–82°N | 29–31°E | Aug 2019 | | | 4 | Ice corer | Bottom section | % | 97±1 | Kohlbach et al. (2021) | C |
| Canadian AA | | 82°N | 62°W | May 2018 | | | 17 | Ice corer | Bottom section | % | 62±9 | Kohlbach et al. (2020) | C |
| Beaufort Sea | | 71°N | 157°W | May 2002 | | | 15 | Ice borer | - | % | 95±2 | Budge et al. (2008) | C |
| Nansen Basin | | 84°N | 78°E | Aug 2012 | | | 1 | Ice corer | Whole core | % | 96 | Kohlbach et al. (2016) | C |
| Amundsen B. | | 82–89°N | 60–131°E | Sep 2012 | | | 9 | Ice corer | Whole core | % | 98±1 | Kohlbach et al. (2016) | C |
| Svalbard | | 80°N | 22°E | Apr, Jun 2007 | | | 9 | Ice corer | Bottom section | % | 91±5 | Leu et al. (2010) | A |
| | | 78°N | 15°E | Apr, May 2017 | | | 29 | Ice corer | Bottom section | % | 100±0 | Leu et al. (2020) | A |
| **Pelagic-POM** | | | | | | | | | | | | | |
| Bering Sea | H | 59–61°N | 174–176°W | Apr–May 2009 | −1.8 | 1.8 | 12 | CTD-Niskin | Chl *a* max | %; µg L$^{-1}$ | 92±1 | Wang et al. (2014) | B |
| | | 56–63°N | 170–180°W | Mar–July 2010 | −2.0 | 7.0 | 53 | CTD-Niskin | Chl *a* max | %; µg L$^{-1}$ | 87±6 | Wang et al. (2014) | B |
| Barents Sea | I | 81–82°N | 28–31°E | May 2021 | −1.8 | −1.3 | 4 | CTD-Niskin | 20m | % | 73±29 | Kohlbach et al. (2022) | C |
| | | 81–82°N | 29–31°E | Aug 2019 | −1.7 | −1.3 | 6 | CTD-Niskin | Chl *a* max | % | 84±8 | Kohlbach et al. (2021) | C |
| Canadian AA | I | 54–80°N | 60–115°W | Jul–Oct 2016 | −1.3 | 8.0 | 65 | CTD-Niskin | Surface, Chl *a* max | % | 75±7 | Marmillot et al. (2020) | C |
| Beaufort Sea | I | 71°N | 157°W | May 2002 | −1.8 | −1.8 | 8 | - | Surface | % | 92±1 | Budge et al. (2008) | C |
| | | 70–71°N | 120–140°W | Aug–Sep 2016 | 2.1 | 8.5 | 6 | CTD-Niskin | Surface, Chl *a* max | % | 65±9 | Marmillot et al. (2020) | C |
| North Bering-/ Chukchi Sea | I | 63–69°N | 165–172°W | Jun 2017 | 1.3 | 6.3 | 33 | CTD-Niskin | Surface, Chl *a* max | %; mg m$^{-3}$ | 85±4 | Nielsen et al. (2023) | C |
| | | 63–69°N | 164–168°W | Jun 2018 | 1.6 | 8.8 | 23 | CTD-Niskin | Surface, Chl *a* max | %; mg m$^{-3}$ | 86±2 | Nielsen et al. (2023) | C |
| | | 68–73°N | 154–168°W | Aug–Sep 2017 | 3.6 | 9.2 | 14 | CTD-Niskin | Surface, Chl *a* max | %; mg m$^{-3}$ | 83±2 | Nielsen et al. (2023) | C |
| | | 63–73°N | 154–172°W | Aug–Sep 2019 | 4.6 | 11.3 | 45 | CTD-Niskin | Surface, Chl *a* max | %; mg m$^{-3}$ | 82±3 | Nielsen et al. (2023) | C |
| West Green-land Sea | I | 63–65°N | 52–55°W | Jun 1999 | −1.0 | 1.0 | 10 | CTD-Niskin | Chl *a* max | % | 80±6 | Reuss and Poulsen (2002) | A |
| | | 63–65°N | 52–55°W | May 2000 | −1.0 | 1.0 | 10 | CTD-Niskin | Chl *a* max | % | 89±2 | Reuss and Poulsen (2002) | A |
| Nansen Basin | L | 81–84°N | 29–87°E | Aug 2012 | −1.8 | −1.0 | 7 | CTD-Niskin | Surface, Chl *a* max | % | 86±5 | Kohlbach et al. (2016) | C |

**TABLE 1** (Continued)

| Arctic region | PP | Lat | Lon | Season | $T_{min}$ (°C) | $T_{max}$ (°C) | No. profiles | Sampling device | Sampling layer/ depth (m) | FA unit | 16 FA (%) mean ± SD | Associated study | Source |
|---|---|---|---|---|---|---|---|---|---|---|---|---|---|
| Amundsen B. | L | 82–84°N | 110–130°E | Sep 2012 | −1.8 | −1.0 | 2 | CTD-Niskin | Surface, Chl a max | % | 92±1 | Kohlbach et al. (2016) | C |
| Svalbard | I | 79°N | 12°E | Apr–May 2003 | −1.5 | −0.5 | 18 | CTD-Niskin | 0, 5, 8, 15, 25, 35 | % | 83±2 | Leu et al. (2006) | A |
|  |  | 79°N | 12°E | May–Jun 2004 | −1.5 | 1.0 | 19 | CTD-Niskin | 0, 5, 8, 15, 25, 35 | % | 87±3 | Leu et al. (2006) | A |
|  |  | 78°N | 15°E | Apr, May 2017 | −2.0 | −1.6 | 12 | CTD-Niskin | 0, 5, 15, 25 | % | 99±1 | Leu et al. (2020) | A |

*Note:* Data sources: A—data are presented in the publication, B—the publication provides a link to the data repository, C—the data were provided by lead/ corresponding author on request. The regional comparison across the studies is based on the profile of 16 key fatty acids (FA) that were analyzed in all studies. The '16 FA (%)' value gives the summed 16 key fatty acids in each of the studies. Surface temperature data (≤10 m water depth) were derived either directly from the publication, from the lead author on request or from satellite data. https://coastwatch.pfeg.noaa.gov/erddap/griddap/NOAA_DHW.html. The pelagic primary productivity was scored as high (H), intermediate/variable (I) or low (L) based on the mean annual primary productivity (g C m⁻² year⁻¹) presented in Frey et al. (2022) (Figure 3a).

Abbreviations: DHA, docosahexaenoic acid; EPA, eicosapentaenoic acid; POM, particulate organic matter.

with Arctic seawater, with or without medium. Sufficient algal biomass for subsequent lipid analysis was grown after 4 weeks for cultures that received media, and after 7 weeks for those without media. At the end of the experiment, two technical replicates were taken from each biological replicate, filtered onto pre-combusted (12 h, 450°C) 25 mm Whatman GF/F filters, freeze dried and stored in aluminum foil at −20°C until FA analysis. All dilutions and final sampling were conducted under sterile conditions, using a laminar flow hood.

## 2.2 | The MOSAiC expedition

The MOSAiC (Multidisciplinary drifting Observatory for the Study of Arctic Climate) expedition represents the first year-round interdisciplinary study of the atmosphere, the sea ice, the ocean, the ecosystem, and biogeochemical processes during the transpolar drift across the CAO, with a unique opportunity for intensive field sampling (Nicolaus et al., 2022; Rabe et al., 2022; Shupe et al., 2022). The observational year was divided into five legs: Leg 1 started on October 4, 2019 with the set-up of the first Central Observatory (CO1) and installations on the research icebreaker *RV Polarstern* north of the Laptev Sea (Knust, 2017; Krumpen et al., 2020). The winter Leg 2 and spring Leg 3 continued the work on CO1, before *RV Polarstern* had to leave the floe, for logistical reasons, on May 16, 2020. The vessel returned to the original ice floe on June 19, 2020, but at a different orientation some hundred meters away. Leg 4 continued the drift with the new CO2 over the summer until the disintegration of the floe in the Fram Strait on July 31, 2020. During Leg 5, *RV Polarstern* travelled back into the ice and started the set-up of CO3 on August 21, 2020, near the North Pole. The third drift ended on September 20, 2020, when the vessel started the return voyage.

### 2.2.1 | Water column sampling

Surface chlorophyll (chl *a*) samples were taken from 11 m water depth via the ship's underway system. Between 2 and 4 L of seawater were filtered in duplicate or triplicate onto GF/F filters and frozen at −80°C until further analyses. Pelagic POM for FA analysis was collected at 2 m and/or the chl *a* fluorescence maximum (chl *a* max, based on CTD fluorescence sensor profiles) via 12 L Niskin bottles attached to the shipboard 24-bottle CTD-rosette (PS-CTD). In the period between mid-March and mid-May, all the water column samples were collected at Ocean City (OC), an in-ice hole 300 m from the ship (OC-CTD), due to the loss of the ice hole alongside the ship (see Rabe et al., 2022). Volumes of 7 to 10 L of seawater were filtered via a vacuum pump (−20 kPA) onto pre-combusted (3 h, 550°C) 47 mm Whatman GF/F filters and stored in aluminium foil at −80°C until further processing.

Additional under-ice sampling took place during MOSAiC Leg 5 from August 26 to September 15, 2020. An in situ automatic pump phytoplankton sampler (PPS; serial number 12697-01; McLane, USA)

was deployed at a depth of 11 m to collect suspended particles. At 2–3 day intervals, 4–6 L seawater were filtered through combusted GF/F filters under different pre-set sample parameters of the PPS.

## 2.2.2 | Sea ice sampling

During Leg 1, areas of first year ice (FYI) and second year ice (SYI) were identified that were safely accessible, relatively homogeneous, and large enough to accommodate repeat visits, potentially for the entire drift. The sites were located away from RV *Polarstern* to minimize human impacts (e.g., artificial lights, traffic, fumes, noise). Cores for biological properties (e.g., chl *a*, taxonomy, trophic markers) were collected using a 9-cm diameter KOVACS Mark II ice corer. Cores were usually sectioned and placed into sterile Whirlpak bags directly inside the ice coring tent under low and/or red-light conditions to minimize artefacts. Small-scale horizontal variability was reduced by pooling 3–4 ice cores, creating a more homogeneous master sample from which related properties were derived. FA profiles of sea ice POM were derived from the two bottom 5 cm intervals (0–5 cm, 5–10 cm) of the pooled ice cores (ECO Pool 1), alongside with samples for pigment analysis (chl *a*, HPLC), POM (POC/PON) and flow cytometry. All pooled samples were melted after the addition of filtered surface seawater (typically 50 mL per 1 cm of core section) to reduce the impact of osmotic stress and cell loss (Campbell et al., 2019; Garrison & Buck, 1986). Ice core sections in bags were melted in the dark at room temperature (18–22°C) and checked every 4–6 h. After complete melting, which took from 12 to 40 h, bags were transferred into dark, temperature-controlled lab containers, and sub-sampled for biological properties under red light to minimize artificial light stimulation of biological activities. The subsamples were filtered via a vacuum pump (−20 kPA) onto pre-combusted 47 mm Whatman GF/F filters and stored in aluminum foil at −80°C until further processing.

A single core was collected for inorganic nutrients and sections were directly melted in the dark. Nutrient samples were pre-filtered through a 0.45 μm membrane filter and either analysed directly on board, or frozen for analysis onshore.

## 2.2.3 | Measurements of PAR (400–700 nm)

The light field above and underneath the sea ice was measured using RAMSES-ACC hyper-spectral radiometers (320–950 nm; TriOS Mess- und Datentechnik GmbH, Rastede, Germany) mounted on the surface control unit and a M500 remotely operated vehicle (ROV, Ocean Modules, Åtvidaberg, Sweden; Katlein et al., 2017). The ROV was lowered into the water through an access hole in the ice and connected to a surface control unit through a tether cable of ~300 m length. The spectral resolution of the radiometer was 3.3 nm, which was interpolated to a common wavelength grid with 1 nm spacing (Nicolaus et al., 2010). The ROV was operated 1–3 times per week with a total of 83 dives (Nicolaus et al., 2022). Once sufficient

sunlight returned in mid-March, comprehensive optical dives were carried out on grids under FYI, SYI, leads, and ridges (Nicolaus et al., 2022). Such transects of continuous measurements, rather than those from single locations, are considered representative of the average PAR experienced by microalgae drifting at a different rate and direction relative to the overlying sea ice (Ardyna, Mundy, Mayot, et al., 2020). For this study, we used the mean incoming PAR and the mean down welling PAR irradiance at water depths between 1.5 and 2.5 m for each dive and present the monthly averages. Data collected in a 2.5 m radius around the ROV access hole were not considered.

## 2.2.4 | Temperature, salinity, and inorganic nutrient analysis

Surface nutrient samples were usually collected at 5.5 m water depth (±1 m) and are presented alongside co-occurring temperature and salinity measurements from bottle CTDs (either PS-CTD or OC-CTD, Tippenhauer et al., 2023a, 2023b). Samples were collected for the measurement of inorganic nutrients (nitrate and nitrite, nitrite, ammonium, silicic acid, phosphate), total dissolved nitrogen and total dissolved phosphorus. Samples were either analysed directly onboard (MOSAiC Leg 1–3) or stored frozen and analysed at the AWI Nutrient Facility (MOSAiC Leg 4–5; experiments with *M. arctica*). Nutrient analyses were carried out using an AA3 Seal Analytical segmented continuous flow auto-analyser following widely used colorimetric techniques (Aminot et al., 2009; Grasshoff et al., 2009; Kirkwood, 1996). The accuracy of analyses was evaluated using KANSO LTD Japan, certified reference materials, with data adjusted accordingly as deemed necessary.

## 2.2.5 | Chlorophyll *a* analysis

Samples were extracted in 90% acetone over night at 4°C and subsequently analyzed on a fluorometer (TD-700; Turner Designs, USA), including an acidification step (1 M HCl) to determine phaeopigments following Knap et al. (1996). During Leg 3, one replicate per event was measured on board, while all other samples were analyzed at AWI after the campaign. No systematic differences between the replicates analyzed onboard and at AWI could be detected, indicating no significant degradation of chl *a* took place during storage and transport.

## 2.2.6 | FA analysis

All filters from the MOSAiC expedition were freeze-dried for 24 h at the AWI and sent to the University of Plymouth, UK for the separation of highly branched isoprenoids (HBI), sterols and FAs. After addition of internal standards for each of the three components (i.e., 23:0 for FA), the filters were saponified with 5% KOH

(70°C; 60 min). Thereafter, non-saponifiable lipids (HBI and sterols) were extracted with hexane (3×2 mL) and purified by open column chromatography (SiO$_2$). FAs were obtained by adding concentrated HCl (1 mL) to the saponified solution and re-extracted with hexane (2×2 mL). The samples were dried under N$_2$ and stored at −20°C in a small amount of hexane until FA analysis. Further steps of the FA analysis were carried out at AWI. Here samples were converted into fatty acid methyl esters (FAME) by using a solution of 3% concentrated sulfuric acid in methanol and heating for 4 h at 80°C (Kattner & Fricke, 1986). Subsequently, FAME were quantified using an Agilent 6890N gas chromatograph (Agilent Technologies, USA) with a DB-FFAP capillary column (60 m, 0.25 mm I.D., 0.25 μm film thickness) supplied with a split-less injector and a flame ionization detector using temperature programming. Helium was used as the carrier gas. FAME were quantified with an internal standard, tricosanoic acid methyl ester (23:0) (Supelco, Germany), that was added prior to lipid extraction. The detection limit based on the certified reference material (Supelco 37 Component FAME mix; Supelco) was 10–20 ng per component. Clarity chromatography software system (version 8.8.0; DataApex) was used for chromatogram data evaluation. FA are presented in shorthand notation, that is, *A:B(n-x)*, where: *A* indicates the number of carbon atoms in the straight FA chain, *B* represents the number of double bonds present, *n* represents the terminal methyl group and *x* denotes the position of the first double bond from the terminal end. Proportions of FA are expressed as mass percentages of TFA content.

## 2.3 | Cross-regional comparison of FA data

For the cross-regional comparison, we included field studies that were carried out since 1999, derived from a region between 60 and 90°N (based on the 'polar region' definition by Colombo et al., 2017), and were permanently or seasonally ice-covered at the time of sampling (Table 1). The sampling protocols of the previous studies largely match those of the MOSAiC expedition, using the bottom section of ice cores for FA analysis of ice POM and the biomass-enriched layers of the water column for pelagic POM. Moreover, the selected studies all present the FA profiles as mass percentage of TFAs and include the following 16 key FA: 14:0, 15:0, 16:0, 16:1(*n*-7), 16:2(*n*-4), 16:3(*n*-4), 16:4(*n*-1), 18:0, 18:1(*n*-9), 18:1(*n*-7), 18:2(*n*-6), 18:3(*n*-3), 18:4(*n*-3), EPA, 22:5(*n*-3) and DHA (Leu et al., 2020). However, some studies identify far more than those 16 FA peaks (i.e., 58 FA, Marmillot et al., 2020). To allow a cross-study comparison of proportional FA, we re-adjusted each dataset to the 16 key FA, which in most cases comprise >85% of the total mass of analysed FAs (Table 1). The regional studies were compared either by sampling month or by sampling season with March–June representing 'spring' and July–September 'summer'. MOSAiC is the only campaign that provided 'winter' data from November to February.

Each study was assigned to a region based on the latitudes and longitudes of the majority of sampling locations. The sampling location(s) may only be representative for a small part of overall region (e.g., 'Barrow' within the 'Beaufort Sea', the Barents Sea northern shelf break in the 'Barents Sea') and only for the specific year of sampling. However, this compilation focusses on reoccurring differences between sea ice and pelagic samples and between shelf regions and deep basins (representing different latitudes), not on regional or temporal differences within individual studies. It would have been desirable to also carry out a cross-regional comparison of the FA concentrations (mg m$^{-3}$) and FA yields (mg m$^{-3}$ day$^{-1}$), but the majority of studies presented the FA data only on a proportional basis (%) (Table 1). Therefore, our study is in line with other data compilations from cultured algae or pelagic and benthic field sampling where FA proportion is the common unit (e.g., Colombo et al., 2017; Galloway & Winder, 2015; Hixson & Arts, 2016; Parzanini et al., 2019).

## 2.4 | Statistics

To interpret the FA data, we used three different statistic approaches: principal components analysis (PCA), box plots with one-way analysis of variance (ANOVA) and linear regression analysis. The PCAs were based on the percentage data of FA profiles, while the box plots present the proportions of EPA or DHA (% of TFA). The FA profiles comprised either 21 FA (cultured algae) or 16 key FA (see explanation under Section 2.3). We used PCAs for four different datasets: the cultured algae, the MOSAiC data, compiled data sets from spring sea ice and pelagic POM, and compiled data sets from summer sea ice and pelagic POM. The PCA on cultured algae was used to illustrate phylogenetic differences within the full FA profiles and the importance of EPA and DHA in driving those variations. The PCA on the MOSAiC data set was used to illustrate monthly differences in the FA profiles and which FA are associated with those seasonal shifts. Finally, the PCAs of the compiled data sets were used to look for similarities and differences in FA profiles from sea ice and pelagic POM derived from Arctic shelf regions versus deep basins. The box plots accompany those PCAs, showing the exact proportions of EPA and DHA. The ANOVA with associated Tukey tests were used for group comparisons, such as between taxonomical groups, seasons, or regions, and results with *p* ≤ .05 were considered significant. Linear regression analysis was used to correlate EPA or DHA proportions with temperature or absolute FA concentrations.

## 3 | RESULTS

### 3.1 | Cultured cold-water diatoms and flagellates have similar summed EPA and DHA proportions

The culture experiments included diatoms (20 strains), flagellates (11 strains) and cyanobacteria (1 strain). The 'flagellates' comprised haptophytes (4), chlorophytes (3), chrysophytes (1), cryptophytes (2), and dinoflagellates (1). The experiments showed that microalgal EPA and DHA proportions are significantly different

between taxonomic groups (Figure 1a,b; ANOVA with Tukey tests, $p < .01$; df = 71, Table S2). When cultured under low temperatures (3–4°C), low light intensity (10 μmol photons m$^{-2}$ s$^{-1}$) and with nutrient-enriched F/2 culture medium, the EPA proportion of diatoms was at least 5% of TFA, reaching maximum values of 25%. Flagellates had significantly lower EPA proportions than diatoms overall, but the two cryptophytes were an exception comprising ~20% EPA (Figure 1b; Table S2). All tested flagellates contained at least 5% DHA, with maximum values of 26%. Overall, the DHA proportions in diatoms were significantly lower than in flagellates, but one diatom (*Nitzschia frigida*) contained 6% DHA (Figure 1b; Table S2). Despite some overlap between diatoms and flagellates in their EPA and DHA production, the two groups were clearly separated on PC1 due to their differences in palmitoleic acid [16:1($n$-7)] which only occurred in high proportions in diatoms (≥20% TFA). The cyanobacterium *Synechococcus* spp. lacked both EPA and DHA but was enriched in 16:1($n$-7) and separated from the diatoms and flagellates on PC2.

Pennate diatoms, centric diatoms and flagellates did not differ in their summed EPA and DHA proportions (Figure S2; ANOVA with Tukey tests, $p = .344$, df = 30).

In parallel to the cultures grown at low temperature and light intensity (3–4°C; 10 μmol photons m$^{-2}$ s$^{-1}$), 19 strains from CCAP were also grown at higher temperature and light intensity (8°C; 20 μmol photons m$^{-2}$ s$^{-1}$). Most strains had equal EPA, DHA proportions in both settings (e.g., *Porosira* spp.) or slightly higher proportions in either the lower (e.g., *Grammonema* spp.) or higher setting (e.g., *Chaetoceros* spp). Only two strains (*Thalassiosira nordenskioeldii* and *Micromonas pusilla*) showed clear differences between the two treatments. However, overall, the EPA and DHA proportions of the 19 strains did not differ significantly between the lower and higher temperature-light combinations (Figure S3; Table S2).

## 3.2 | *M. arctica* EPA proportions decline with low nutrient and light availability

The diatom *M. arctica* showed an up to 3-fold difference in EPA proportion depending on its culture conditions after allowing 4–7 weeks of acclimation, while the DHA proportions were consistently low (≤1% TFA). One of the six treatments represented the strain's long-term maintenance conditions with low temperature (1°C), low light (10 μmol photons m$^{-2}$ s$^{-1}$) and nutrient-enriched culture medium (F/20 medium). In this setting, *M. arctica* had a moderate EPA proportion of 9% (Figure 1c). The EPA proportion increased significantly to >11% when the light intensity was raised to 100 μmol photons m$^{-2}$ s$^{-1}$ (Figure 1c; ANOVA with Tukey tests, $p < .01$, df = 22). If light intensity and temperature were increased, the EPA proportion remained unchanged at 3°C (9% EPA) but was significantly reduced at the warmer 6°C treatment (7% EPA) (Figure 1c). Lowest EPA proportions were recorded when *M. arctica* was kept for 7 weeks without nutrient-enriched culture medium. However, there was a significant difference in the EPA proportion depending on whether the nutrient starvation was combined with a high light intensity (100 μmol photons m$^{-2}$ s$^{-1}$; EPA 6%) or low light intensity (10 μmol photons m$^{-2}$ s$^{-1}$; EPA 3.5%).

## 3.3 | A strong seasonal cycle in the EPA and DHA proportions of sea ice and pelagic POM

During the year-long MOSAiC expedition (Figure 2a,b), incoming PAR changed by three orders of magnitude from complete darkness in winter to maximum values of ~1000 μmol photons m$^{-2}$ s$^{-1}$ in July (Figure 2c). At the same time, the surface water temperature remained constant at $-1.7 \pm 0.1$°C (Figure 2c,d). The macronutrients nitrate and silicate showed more complex cyclicity, partly due to the long-distance drift across water masses of different origin and nutrient inventories, which coincided with the seasonal build-up of algae biomass (Figure 2e–g). However, while the nitrate concentrations in sea ice were consistently low (<1 μmol L$^{-1}$), those in the upper water column included high as well as very low concentrations and an inverse relationship between nitrate and silicate (Figure 2e,f). Pelagic microalgae reached bloom concentrations of ≥1 μg chl $a$ L$^{-1}$ only in June and July 2020 (Figure 2g). The TFA concentrations were an order of magnitude higher in bottom sea ice than in biomass-enriched layers of the water column, with maximum values of 220 and 28 mg m$^{-3}$, respectively (Figure 2h). In water column samples, there was a strong positive relationship between the proportions of EPA or DHA and the TFA concentration (EPA: $R^2 = .44$, DHA: $R^2 = .34$), while in sea ice samples, the positive relationship was weaker for EPA ($R^2 = .19$) and non-significant for DHA (Figure 2h; Figure S4). For the following cross-regional comparisons, only the FA proportions are considered, as this is the common FA unit in the previous Arctic studies (Table 1).

EPA and DHA proportions in sea ice and pelagic POM, sampled during MOSAiC, showed differences across the year (Figure 3a,b; ANOVA with Tukey tests, $p < .01$, sea ice POM df = 56, pelagic POM df = 59). Samples from summer versus winter/spring are separated on PC1, and those from early versus late summer on PC2 (Figure 3a). Winter/spring (November–May; MOSAiC Leg 1–3) samples are associated with higher proportions of saturated FA (e.g., 18:0, 16:0) while those from early summer (June/July; MOSAiC Leg 4) are associated with diatom-marker FA [e.g., 16:1($n$-7), C$_{16}$ PUFA, EPA] and those from late summer (August/September; MOSAiC Leg 5) with flagellate-marker FA (e.g., C$_{18}$ PUFA, DHA). The seasonal peak of EPA proportions occurred in June/July in sea ice and in July in pelagic POM, while the DHA proportions showed little variation in sea ice and peaked in August in pelagic POM (Figure 3b).

As data from the MOSAiC drift will have been influenced by both seasonal and regional transitions, especially the pelagic POM (see Figure 2b for the drift trajectory), we also present a pelagic spring–summer time-series from a single region, the Bering Sea, with pelagic POM sampled in 2009 and 2010 (Figure 3c; Table 1). In line with the
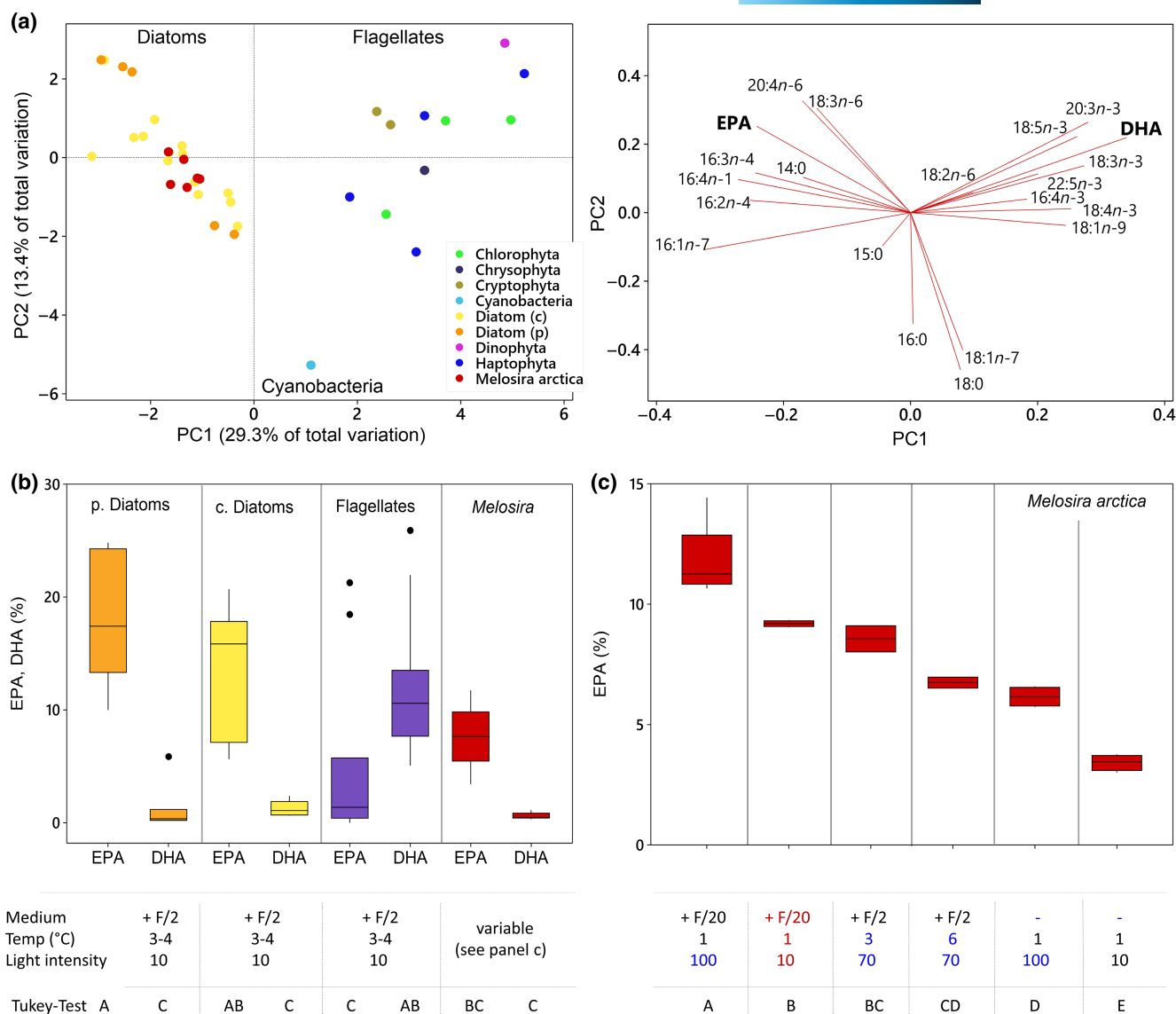
**FIGURE 1** Cultured cold-water microalgae: Phylogenetic and environmentally driven differences in the EPA and DHA proportions. (a) Principal component analysis of fatty acid percentage data. Score- (left) and loading plot (right) for diatoms (20 strains), flagellates (11 strains) and cyanobacteria (1 strain, *Synechoccocus* spp.); showing that EPA is associated with diatoms and DHA with flagellates, while the cyanobacterium lacks EPA and DHA. (b) Box plots of EPA and DHA proportions (% of total fatty acid) in pennate (p) diatoms ($n=7$), centric (c) diatoms ($n=13$) and flagellates ($n=11$) represent phylogenetic differences under standardized culturing conditions, while the box plots for *Melosira arctica* represent environmentally induced differences with one strain grown under different culturing conditions. Means that do not share the same letter (A, B, C) are significantly different, ANOVA with Tukey test ($p<.01$). (c) Box plot of EPA proportions in *M. arctica* cultured under six different combinations of temperature, light intensity and nutrient supply ($n=4$). The red labelling indicates the long-term maintenance conditions and the blue labelling the parameter(s) that was (were) changed in each modified set-up (Figure S1). 'Pennate diatoms' include the genera *Nitzschia*, *Navicula*, *Pseudo-nitzschia*, *Synedropsis*, *Grammonema*. 'Centric diatoms' include the genera *Attheya*, *Chaetoceros*, *Melosira*, *Porosira*, *Thalassiosira*, and 'Flagellates' include the genera *Micromonas*, *Pyramimonas*, *Phaeocystis*, *Emiliania*, *Isochrysis*, *Polarella*, *Rhodomonas*, *Baffinella*, *Dinobryon* (further details in Table S1). DHA, docosahexaenoic acid; EPA, eicosapentaenoic acid.

observations from MOSAiC, the Bering Sea dataset shows (1) strong seasonal differences in EPA and DHA proportions, (2) an earlier peak in EPA than DHA proportions, (3) lower EPA and DHA proportions in early spring (March), compared to the seasonal maximum in later spring or summer. However, during the MOSAiC drift, the timing of the seasonal peak was 1 month later for the DHA and 2–3 months later for the EPA proportions, compared to the low-latitude Bering Sea.

## 3.4 | Sea ice and pelagic POM show no systematic differences in EPA and DHA proportions

Studies that have simultaneously sampled EPA and DHA proportions in sea ice and pelagic POM are relatively rare and give disparate results as a function of season (Figure 4a–d, ANOVA with Tukey tests, $p<.01$, spring df = 100, summer df = 113). Four spring studies (March–May) found higher EPA and DHA proportions in sea

**(a)** Arctic

BeS-Bering Sea
ChS-North Bering- & Chukchi Sea
BfS-Beaufort Sea
CAA-Canadian Arctic Archipelago
WGS- West Greenland Shelf
BaS-Barents Sea
Sv-Svalbard
NB-Nansen Basin
AB- Amundsen Basin
CAO-Central Arctic Ocean

**(b)** Central Arctic Ocean (CAO)
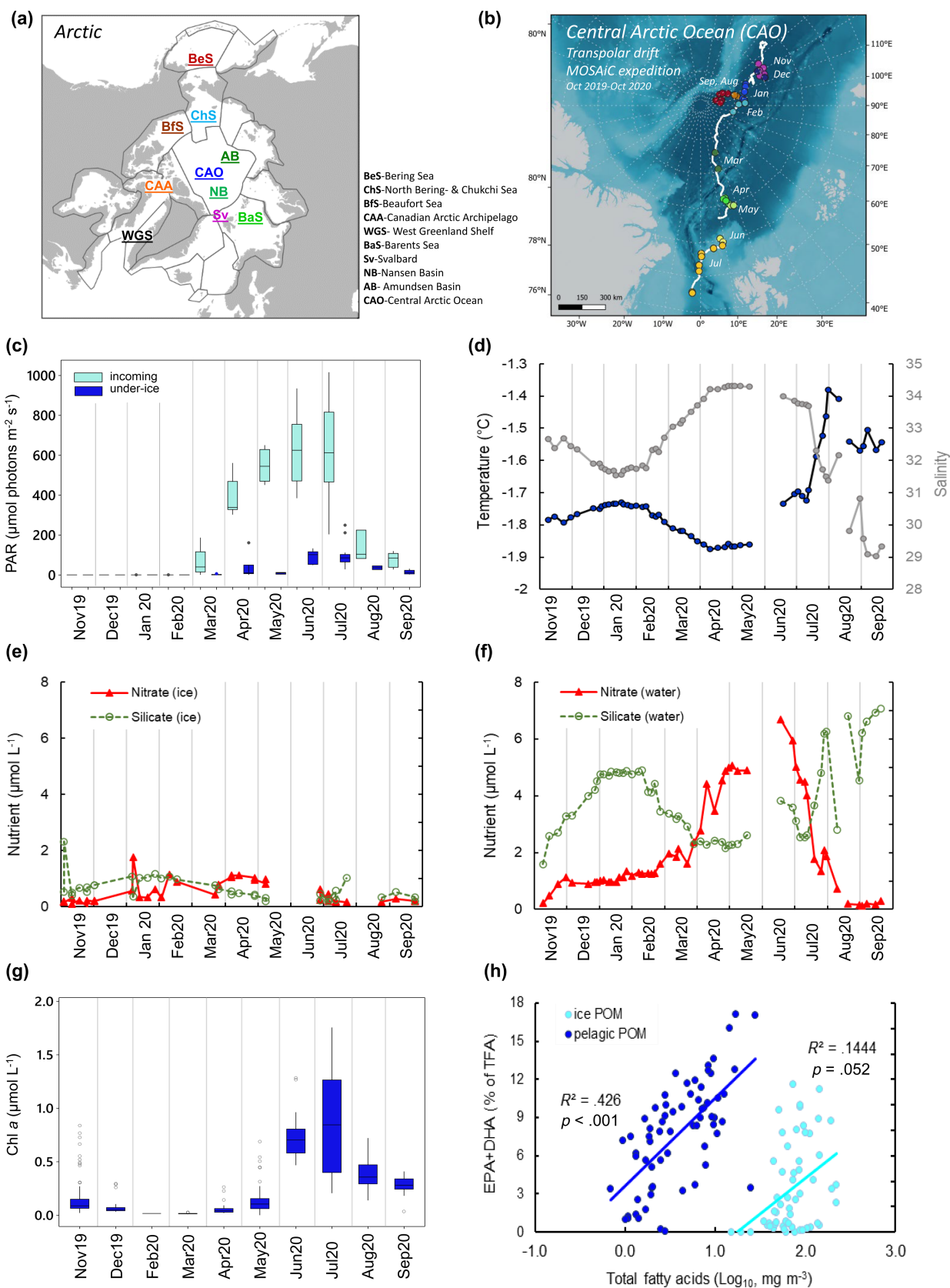Transpolar drift
MOSAiC expedition
Oct 2019-Oct 2020

**FIGURE 2** Arctic study regions and the MOSAiC expedition (October 2019–October 2020): Locations and environmental conditions. (a) Location of Arctic regions that were sampled for this data compilation. Boundaries of large marine ecosystems of the Arctic are depicted (PAME, 2014). (b) Trajectory of the MOSAiC expedition (white line). Coloured dots indicate sampling sites of sea ice- and pelagic POM for FA analysis. (c) Mean photosynthetically active radiation (PAR) measured ~1 m above sea level (=incoming PAR) and under sea ice (=transmitted PAR). (d) Temperature (black) and salinity (grey) from bottle CTD at nutrient sampling depths (5.5 ± 1 m depth). (e) Nitrate and silicate concentrations in bottom sea ice. (f) Nitrate and silicate concentrations in surface waters (5.5 ± 1 m depth). (g) Chlorophyll *a* concentration in surface waters collected from ship's sea water intake at 11 m water depth. (h) Relationship between the summed EPA, DHA proportions and the total FA concentrations in sea ice or pelagic POM (plots of individual FA in Figure S4). DHA, docosahexaenoic acid; EPA, eicosapentaenoic acid; FA, fatty acid; POM, particulate organic matter.

ice than in pelagic POM (Figure 4a,b), while four summer studies (May–September) found the reverse (Figure 4c,d). Samples collected during MOSAiC show significant differences in the DHA proportions in sea ice- and pelagic POM, while the EPA proportions were similar (Figure 4a,c).

For the spring scenario, sea ice and pelagic POM were separated on PC1, with sea ice samples being associated with higher EPA and DHA proportions and pelagic samples with higher proportions of saturated FA (18:0, 16:0, 15:0) (Figure 4b). At the same time, sea ice and pelagic samples from the Bering Sea were separated from those collected at Svalbard on PC2. The Svalbard samples were associated with high proportions of palmitoleic acid [16:1(*n*-7)], while the Bering Sea samples had high proportions of oleic acid [18:1(*n*-9)] and linoleic acid [18:2(*n*-6)] in both sea ice and pelagic POM.

In the late spring–summer scenario, sea ice and water samples were separated on PC2 (Figure 4d). This time, the pelagic samples were associated with higher EPA and DHA proportions, and the sea ice samples with higher proportions of saturated FA or 16:1(*n*-7). PC1 separated the four different study regions, with samples from MOSAiC being associated with high proportions of 18:1(*n*-9) and 18:2(*n*-6), and those from the Beaufort Sea with high 16:1(*n*-7).

## 3.5 | Regional comparisons reveal unexpectedly low EPA and DHA proportions during MOSAiC

For a regional comparison of EPA and DHA proportions, the MOSAiC dataset was assessed alongside ~470 POM profiles from 13 previously published studies. The data were divided into four categories: (1) sea ice-spring; (2) sea ice-summer; (3) pelagic-spring, (4) pelagic-summer. FA profiles of sea ice-summer have only been sampled in four regions, with stations at the shelf break or in the Arctic basins, and EPA and DHA proportions being low and not significantly different between regions (Figure 5a,b; ANOVA with Tukey tests, EPA *p* = .519, DHA *p* = .432, df = 30). In the other categories, samples from MOSAiC were significantly lower in EPA proportions than those from most other regions (ANOVA with Tukey tests, *p* < .05, sea ice-spring df = 113, pelagic-spring df = 202, pelagic-summer df = 194). In contrast, the inflow shelf or shelf break regions of the Bering Sea and Barents Sea had the highest EPA and DHA proportions in all categories, except for the DHA proportion in sea ice-spring that was highest in the Canadian Arctic Archipelago (CAA). While the

pelagic-summer samples from MOSAiC, that derived from the Fram Strait and North Pole region, showed low EPA and DHA proportions, samples from the Nansen Basin collected during exceptionally low sea ice-extent in summer 2012 (Kohlbach et al., 2016) contained significantly higher DHA proportions (Figure 5b, ANOVA with Tukey tests, *p* < .05).

## 4 | DISCUSSION

Polar regions, and in particular sea ice habitats, are often perceived as hotspots of long-chain omega-3 FAs production due to low temperatures and the abundance of bloom-forming diatoms (Colombo et al., 2017; Jónasdóttir, 2019; Søreide et al., 2010). Our results from the Arctic indicate more diverse scenarios of highly variable algal EPA and DHA proportions in both sea ice and the water column. Contrary to our initial hypothesis, we predict algal EPA and DHA proportions to increase rather than decrease in large parts of the ice-free Arctic. Regarding the five mechanisms that are proposed to lead to lower microalgal EPA, DHA proportions in a future Arctic (see Section 1), our observations are as follows:

1. *Loss of ice algae*: Cultures of cold-water pennate and centric diatoms did not show systematic differences in their EPA proportions. In line with seasonal changes in light and nutrient availability in the two habitats, EPA and DHA proportions first peaked in sea ice and then in pelagic POM, but the maximum values were similar.

2. *Increased irradiance*: The *M. arctica* culture showed lower EPA proportions at a light intensity of 10 compared to 100 μmol photons m$^{-2}$ s$^{-1}$. In the field, lowest EPA proportions in sea ice and pelagic POM occurred at the end of the dark winter season.

3. *Reduced nutrient concentrations*: Without the supply of culture medium, the EPA proportions in *M. arctica* dropped by 50% over a 7-week period. In the CAO, EPA and DHA proportions of microalgae are currently low and have therefore the potential to increase where nutrient and light levels become more favourable.

4. *Community shifts towards non-diatoms*: In the culture experiments, diatoms contained highly variable proportions of EPA and were not per se a superior source of omega-3 FA over non-diatom species, including those that become increasingly present in the Arctic under climate change. Across multiple regions of the Arctic, open waters in summer (July–September) were characterized by
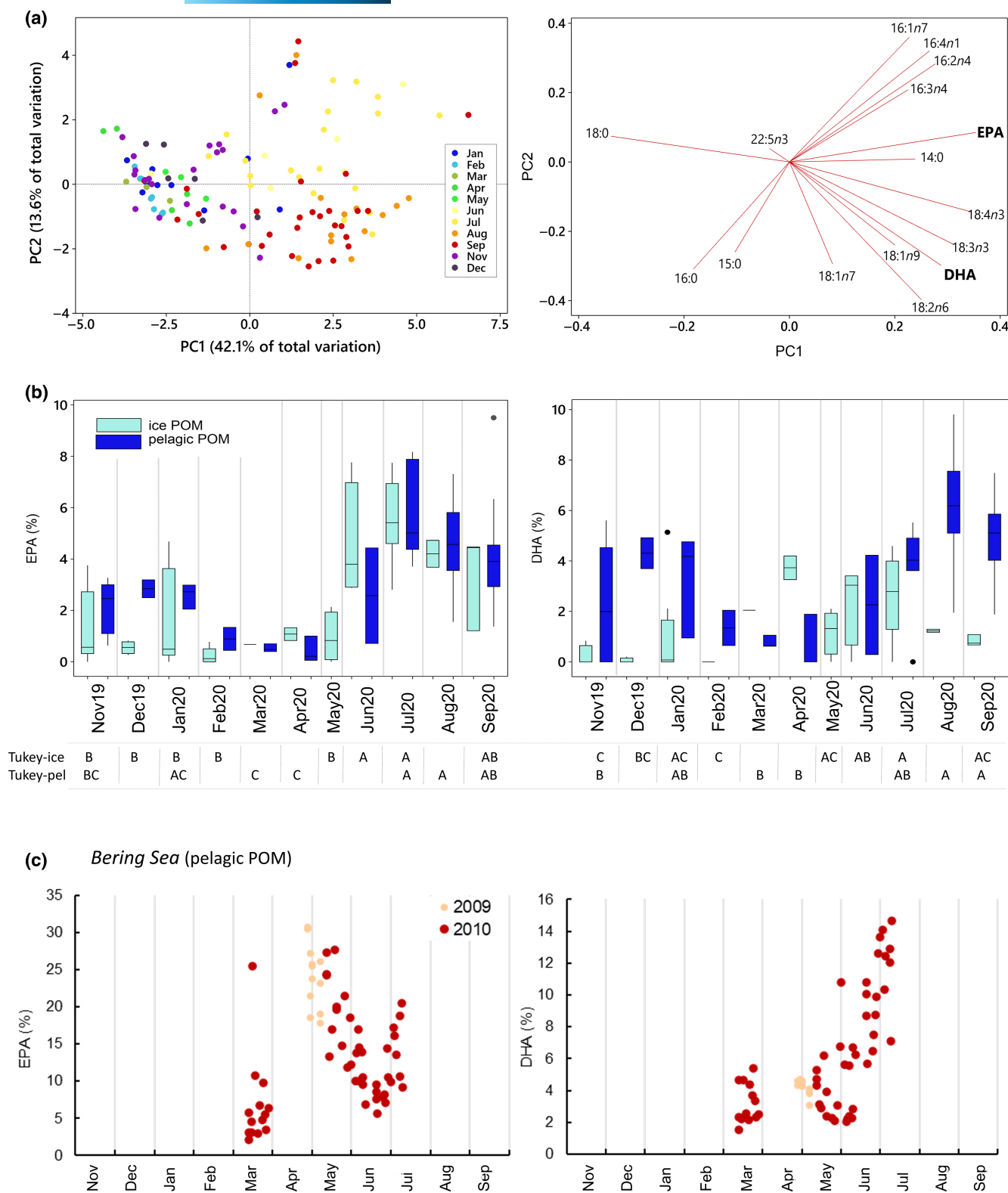
**FIGURE 3** Seasonal cycle of EPA and DHA proportions in sea ice and pelagic POM. (a) MOSAiC: Principal component analysis of FA percentage data from sea ice and pelagic POM with the scores of different months (left panel) and FA loadings (right panel). (b) MOSAiC: Monthly average EPA and DHA proportions (% total fatty acid) in POM from sea ice and pelagic POM. Means that do not share the same letter (A, B, C) are significantly different, ANOVA with Tukey test ($p < .01$). (c) Bering Sea: Spring–summer transition in EPA and DHA proportions of pelagic POM (Data source info in Table 1). DHA, docosahexaenoic acid; EPA, eicosapentaenoic acid; FA, fatty acid; POM, particulate organic matter.

high algal DHA proportions, indicating an increasing role of late flagellate blooms.

5. *Rising temperatures*: Across 19 cold-water strains tested in the laboratory, a 4°C increase in temperature combined with a $10\,\mu mol\,photons\,m^{-2}\,s^{-1}$ increase in light intensity did not cause a significant change in their EPA and DHA proportions. In the field, highly variable EPA and DHA proportions were observed against a constant background of near-freezing temperatures. In the Bering and Chukchi Sea, where summer temperatures in surface waters rise to over 10°C, DHA proportions in pelagic POM actually increased, rather than decreased, with temperature (Figure S5). The low EPA and DHA proportions in microalgae and zooplankton from the coldest CAO indicate that components other than EPA and DHA may contribute to homeoviscous adaptation (DeLong & Yayanos, 1985; Guschina & Harwood, 2009; Sinensky, 1974) and that wax ester phase transition from liquid to gel forms can be tolerated (Sakinan et al., 2019).

How nutrients and light may limit EPA and DHA production in the ice-covered CAO, and possibly in other global regions, is further examined below.

## 4.1 | Lack of light and/or nutrients results in low EPA proportions in the CAO

In the CAO, sea ice and pelagic POM are characterized by low EPA proportions of ≤10% TFA compared to 20% or 30% EPA found in Arctic shelf regions further South, which may infer regional differences in the relative abundance of EPA-producing algae. With the lack of taxonomic information for the compiled dataset, we used the simultaneously analyzed biomarker FA, 16:1(*n*-7), which is prominent in diatoms (Figure 1a, Dalsgaard et al., 2003) and a predictor of diatom total abundance (Nielsen et al., 2023). About one-quarter of all MOSAiC samples contained no or low proportions of this diatom biomarker (Figure 6). The low diatom abundance might be caused by a tight coupling of autotrophic and heterotrophic production in polar waters of the CAO (Flores et al., 2019), especially during the winter months when a large part of the MOSAiC sampling took place. However, the regional comparison also shows that for higher proportions of 16:1(*n*-7), the MOSAiC samples contained less EPA than samples from the shelf regions (Figure 6). Some of this 'additional' EPA in Arctic shelf regions may derive from non-diatom sources, such as Chrysophyceae or certain macroalgae (Graeve et al., 2002; Jónasdóttir, 2019), that are lacking in the CAO. However, the simultaneous increase of 16:1(*n*-7) and EPA over the first third of the dome-shaped relationship, suggests a common source of the two components, at least in the MOSAiC, Bering Sea and CAA samples (Figure 6). We therefore conclude that diatoms in the CAO have a lower potential of EPA production than their southern counterparts, due either to their specific taxonomic composition or to the prevailing environmental conditions. The lower EPA proportions are also seen in the next trophic level

(e.g., the copepod *Calanus hyperboreus*, Figure 6f), which implies that selective feeding and bioaccumulation cannot overcome the EPA deficiency in the CAO primary producers.

In our culture experiments, we found five-fold differences in EPA proportions between different diatom strains grown under the same environmental conditions and near four-fold differences for a single strain of *M. arctica* grown under a range of environmental conditions (Figure 1b,c; Figure S3). There was no systematic difference in the EPA proportions of pennate and centric diatoms, and even strains of the same species or genus showed variability. The strong effect of the environmental setting, time since strain isolation and phase of their growth curve on EPA production (Hamilton et al., 2015; Pond & Harris, 1996), makes it difficult to establish taxonomic differences from cultured algae. Field studies, where FA profiles are analyzed on individual algae strains, may clarify whether taxonomic differences in EPA production are contributing to systematically lower EPA proportions in the CAO. Without such evidence, we focus on the potential role of environmental differences between the CAO and Arctic shelf regions.

In the culture experiments with *M. arctica*, we tested the effect of temperature, light intensity and nutrient supply on EPA proportions and found a response to all three factors. Lack of nutrients had the strongest effect on the EPA proportions, which dropped from over 11% to 3% EPA after several weeks of nutrient deprivation. This decrease of EPA is in line with the principal response of most algae to nutrient limitation, where cell growth and membrane synthesis slows, and FA are mainly stored as saturated and mono-unsaturated FA in triacylglycerols (Guschina & Harwood, 2009; Thompson, 1996). At the same time, the proportion of galactolipids, typical constitutes of thylakoid membranes and enriched in EPA and DHA, decreases (Alonso et al., 2000; Lynn et al., 2000).

Assessing nutrient limitation of algae in situ is challenging due to interdependent nutrient stoichiometry and co-effects of light or temperature. During MOSAiC, the ice floe drifted from the Amundsen to the Nansen Basin and Fram Strait; regions that are influenced by different water masses, with different nutrient inventories and ratios (Flores et al., 2019; Laukert et al., 2022; Tuerena et al., 2021). Therefore, the accumulation of microalgal biomass in spring (Figure 2g) coincided with an increase rather than decrease in nitrate concentrations from March to June as the ice floe reached the nitrate-replenished Atlantic-influenced water masses with higher salinity (Figure 2b,d,f). However, two observations point to potential nutrient limitation during MOSAiC and could therefore explain the unexpectedly low EPA proportions in POM: firstly, in the Atlantic-influenced water masses, the silicate concentrations reached a minimum of ~$2\,\mu mol\,L^{-1}$ in surface waters and $0.2\,\mu mol\,L^{-1}$ in bottom sea ice, with nitrate-to-silicate molar ratios of up to 2 in surface waters and 5 in sea ice. Such depleted silicate concentrations and nitrate-to-silicate ratios >1 can drastically reduce silicate uptake by diatoms, limit their growth and shift the microalgae assemblage towards flagellates (Ardyna, Mundy, Mills, et al., 2020; Krause et al., 2019; Oziel et al., 2017). Secondly, the Arctic surface waters near the North Pole had low nitrate concentrations of ~$0.9\,\mu mol\,L^{-1}$ in winter (MOSAiC, Leg 2) and <$0.2\,\mu mol\,L^{-1}$ the following summer (MOSAiC, Leg 5), with
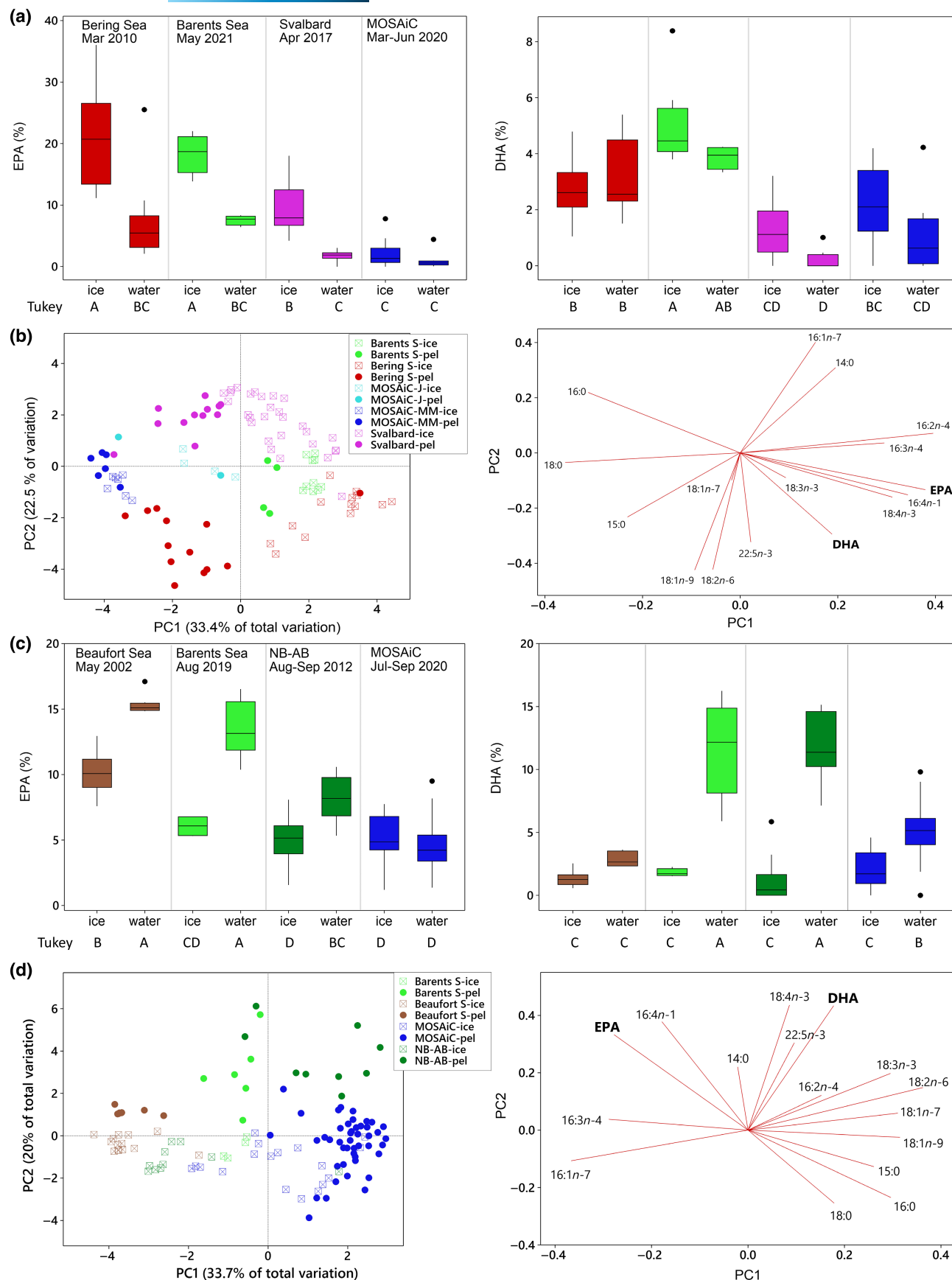
**FIGURE 4** Comparison of EPA and DHA proportions in simultaneously sampled sea ice and pelagic POM. Sampling events, where sea ice (a, b) or pelagic POM (c, d) had higher proportions of EPA or DHA (% of total fatty acid). (a, c) EPA and DHA box plots. Means that do not share the same letter (A, B, C) are significantly different, ANOVA with Tukey test ($p < .01$). (b, d) Principal component analysis of FA percentage data with the scores of sea ice and pelagic POM samples (left) and fatty acid loadings (right). DHA, docosahexaenoic acid; EPA, eicosapentaenoic acid; FA, fatty acid; J, June; MM, March to May; NB-AB, Nansen Basin-Amundsen Basin; POM, particulate organic matter.

**FIGURE 5** Regional differences in EPA and DHA proportions in sea ice and pelagic POM. (a) EPA (% of TFA); (b) DHA (% of TFA). Arctic shelf and shelf-break regions include Bering Sea (BeS, red), Barents Sea (BaS), Canadian Arctic Archipelago (CAA), Beaufort Sea (BfS), Svalbard (Sv), North Bering-/Chukchi Sea (ChS), and West Greenland shelf (WGS). Deep Arctic basins include Nansen Basin (NB), Amundsen Basin (AB) and MOSAiC (blue). The data are grouped into four categories: (1) spring-sea ice, (2) spring-pelagic, (3) summer-sea ice, (4) summer-pelagic. Spring: March–June; Summer: July–September. For each season, the regions are sorted in descending order of the median EPA or DHA proportion. For cross-regional comparison, original FA datasets were normalized to a core set of 16 fatty acids as described in Section 2. Means that do not share the same letter (A, B, C) are significantly different, ANOVA with Tukey test ($p < .01$). DHA, docosahexaenoic acid; EPA, eicosapentaenoic acid; POM, particulate organic matter; TFA, total fatty acid.
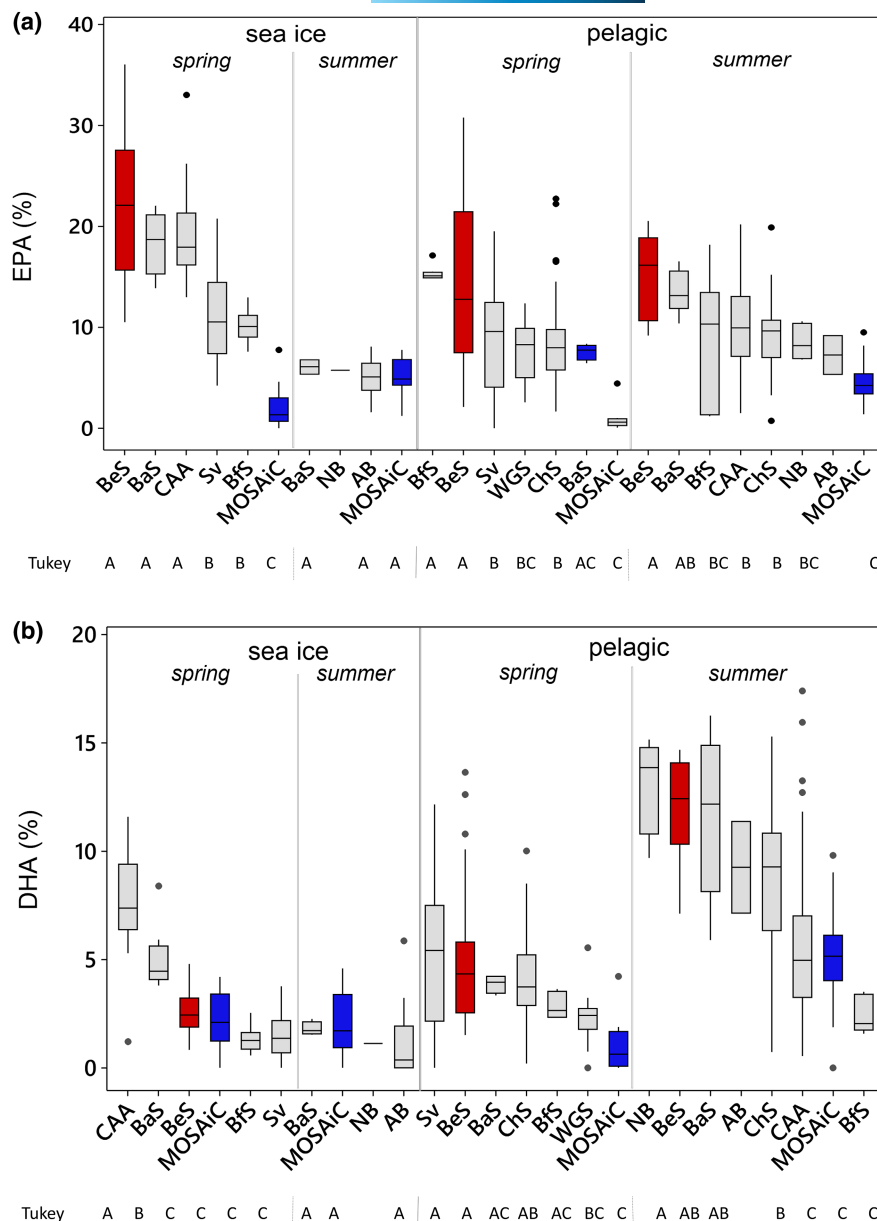
sea ice containing low concentrations ($\leq 0.2\,\mu mol\,L^{-1}$) during both seasons. We therefore suggest that the low EPA proportions per diatom biomarker 16:1(*n*-7), observed during MOSAiC, are at least partly caused by either low silicate or low nitrate concentrations and high nitrate-to-silicate ratios, especially in sea ice.

In the culture experiments with *M. arctica*, an increase in light intensity from 10 to $100\,\mu mol\,photons\,m^{-2}\,s^{-1}$ led to a moderate increase in EPA proportion from 9% to over 11% (Figure 1c). Previous studies have described two opposite responses of microalgae to low light intensity: either EPA proportions rise to enhance membrane fluidity, thylakoid stacking and the velocity of the electron flow (Mock & Kroon, 2002) or EPA proportions sink to reduce membrane fluidity, and therefore proton leakage and metabolic costs (Raven et al., 2000). Which of these responses is used, seems to depend on species-specific light acclimation strategies and differences in light optima (Clegg et al., 2003; Falkowski & Owens, 1980; Wacker

et al., 2015, 2016 and references therein). However, during low light conditions in Arctic spring, EPA proportions are higher in the more-illuminated sea ice POM compared to the less-illuminated pelagic POM (Figure 4a), which suggests that algae respond here to light limitation with an EPA reduction, in line with our findings in the culture experiments. During MOSAiC ROV dives, average PAR of $\geq 10\,\mu mol\,photons\,m^{-2}\,s^{-1}$ below the sea ice ($\geq 1.5\,m$ thick) was encountered from April to September, while PAR of $\geq 100\,\mu mol\,photons\,m^{-2}\,s^{-1}$ occurred only in June and July. Using the *M. arctica* response in culture experiments as a benchmark, light intensities below $10\,\mu mol\,photons\,m^{-2}\,s^{-1}$ may have limited pelagic EPA production in the CAO during large parts of the year.

*Melosira arctica*'s EPA proportions also showed a negative response to a 2 or 5°C temperature rise after 4-weeks of acclimation. This is in line with previous findings that diatom EPA proportions are reduced at higher temperatures (Guschina & Harwood, 2009; Hixson
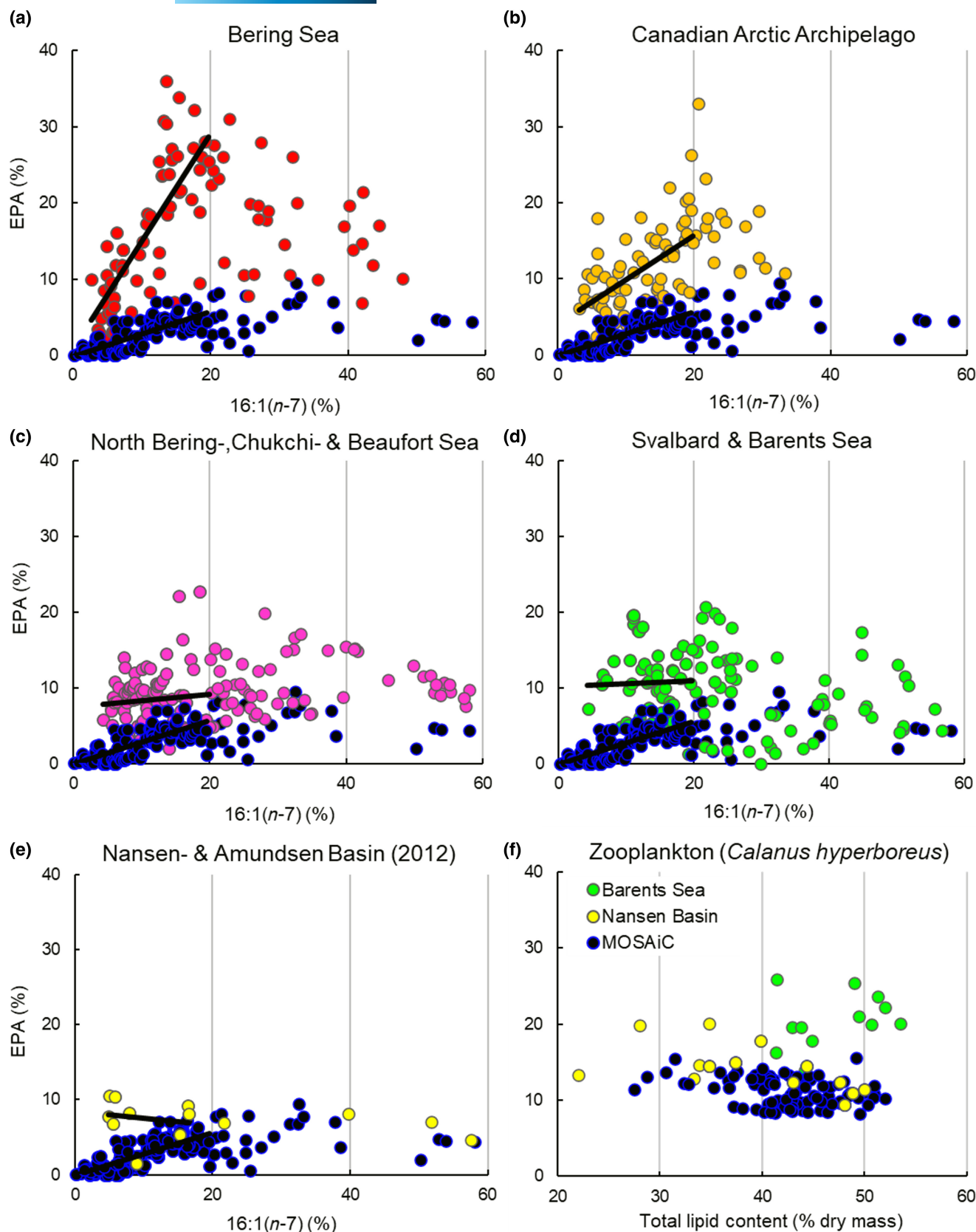
**FIGURE 6** Regional differences in the co-occurrence of EPA and 16:1(*n*-7) in sea ice and pelagic POM, or EPA and total lipid content in zooplankton. (a) Bering Sea (red dots). (b) Canadian Arctic Archipelago (orange dots). (c) North Bering-, Chukchi- and Beaufort Sea (pink dots). (d) Svalbard and Barents Sea (green dots). (e) Nansen- and Amundsen Basin (yellow dots). (f) The copepod *Calanus hyperboreus* from the Barents Sea (green) and Nansen Basin (yellow). The MOSAiC data are plotted as blue dots in all panels. The interpretation of Panel (a–e) is supported by the culture experiments with the diatom *Melosira arctica* (Figure S6). EPA, eicosapentaenoic acid; POM, particulate organic matter.

& Arts, 2016). However, for our field data compilation, temperatures were uniformly low for all sea ice samples, and for all pelagic samples from the MOSAiC and Arctic shelf regions in spring (Figure 2d; Table 1). For studies that encountered higher temperatures in summer (e.g., 11.3°C in the North Bering-Chukchi Sea in August/September 2019), the relationships between EPA proportion and in situ temperature did not reveal any significant trend (Figure S5). We therefore conclude that the higher EPA proportions in Arctic shelf regions compared to the CAO were caused by higher nutrient and light availability rather than higher summer temperatures.

## 4.2 | Microalgae EPA and DHA proportions in an increasingly ice-free Arctic

Arctic primary productivity shows a number of re-occurring patterns, such as low to no primary production in winter, the seasonal peak rising and ceasing first in ice algae and then in pelagic algae (Arrigo, 2017), later microalgal blooms in higher compared to lower latitudes (Ardyna, Mundy, Mayot, et al., 2020), potential secondary microalgae blooms in regions with long open water seasons (Ardyna et al., 2014), and lower primary productivity in the Arctic Basins compared to shelf regions (Matrai et al., 2013). The EPA and DHA proportions in POM largely resembled these patterns including the seasonal cycle (Figure 3), the different phenology in sea ice versus water column (Figure 4), and the differences between eutrophic and oligotrophic regions (Figure 5). These analogues might reflect the fact that during the highly productive season, a larger POM fraction is composed of living algae enriched in EPA and DHA than during the less-productive season, when EPA and DHA pools are not replenished and reach the lowest proportions by the end of winter, due to grazing, sedimentation, decay and turnover. We therefore suggest that environmental conditions that support high primary productivity in a changing Arctic also lead to high EPA and DHA proportions in POM.

A key factor driving primary production is the availability of nutrients. Arctic sub-regions range greatly in trophic status from eutrophic to oligotrophic, with climate change further amplifying such differences (Frey et al., 2022). Over shallow inflow shelves (eastern Bering Sea, Barents Sea, Chukchi Sea), the nutrient supply has generally increased, first, due to enhanced advective nutrient input from lower latitudes and second, due to strong nutrient replenishment during winter when reduced sea ice cover allows convective and storm-driven mixing (Juranek, 2022). In contrast, in the Central Arctic, enhanced melt water input further strengthens the vertical stratification and therefore weakens the replenishment of nutrients via storm events (Juranek, 2022). The EPA and DHA proportions in POM reflect these regional differences in nutrient availability with high EPA and DHA proportions in the eutrophic shelf regions and low proportions in the oligotrophic CAO (Figures 5 and 6). However, over longer timescales, when the sea ice cap has completely melted during summer, a uniform surface mixed layer may develop with enhanced wind-driven nutrient supply from deeper waters and lateral fluxes of shelf-derived material (Ardyna et al., 2017; Kipp et al., 2018). Under

such conditions, the surface CAO may evolve into a more productive region, with higher algal EPA and DHA proportions.

A further factor that is likely to affect the EPA and DHA proportions in a future Arctic is the taxonomical composition of the primary producer community, with diatoms being key EPA and flagellates DHA producers (Figure 1a, Dalsgaard et al., 2003). For the 32 cold-water algae strains we tested in culture experiments, there was no systematic difference in the combined EPA and DHA proportions of flagellates versus diatoms, which underlines that flagellates can be of equally high nutritional value as diatoms (Galloway & Winder, 2015; Jónasdóttir, 2019; Peltomaa et al., 2017; Pond & Harris, 1996). In line with these results from culture experiments, the field data reveal high DHA proportions in pelagic POM across Arctic regions in late summer (on average 10%–15%, Figure 5). With the spatial and temporal reduction in ice cover and enhanced atmospheric forcing resupplying nutrients, late summer blooms become increasingly prominent in the Arctic (Ardyna et al., 2014; Juranek, 2022). Our results, showing positive correlations between DHA proportions and temperature (Figure S5), suggest that flagellates can benefit from warmer, more stratified, surface waters. Such late summer pulses of DHA-rich food can benefit zooplankton recruitment by lengthening their growing and reproductive season and by providing a depot of nutrition for the winter-active part of the populations (Flores et al., 2023; Hobbs et al., 2020; Tremblay et al., 2011). Without doubt, the spring diatom bloom will remain the major annual primary production event in the Arctic (Ardyna et al., 2013) and this study shows that EPA and DHA proportions are high, irrespective of their production in sea ice or the upper water column, as long as the nutrient supply is sufficient.

Overall, we conclude that relatively low algal EPA and DHA proportions, that might be typical for the permanently ice-covered Arctic, are likely to increase under climate change, where primary production is also increasing.

## 4.3 | Implications for the Arctic food web and predictions of global EPA and DHA productions

In large parts of the Arctic, warming and sea ice loss coincide with increased light and nutrient availability and therefore overall increased primary production (Ardyna & Arrigo, 2020; Lewis et al., 2020; Terhaar et al., 2021). The EPA and DHA proportions in those primary producers are either already high (e.g., Bering Sea) or likely to increase (e.g., CAO), which will benefit secondary production in the Arctic. The polar regions are the only global regions where both phytoplankton and zooplankton stocks are predicted to increase over this century (Tittensor et al., 2021). On the downside, this 'greener' Arctic is inevitably linked to the loss of one of Earth's unique habitats—Arctic sea ice, to the loss of biodiversity and human traditions, and to massive implications for our climate.

For the rest of the global ocean, reductions in phytoplankton biomass, and amplified reductions in zooplankton are projected, especially in the north Atlantic (Tittensor et al., 2021). With an expanding human population and its reliance on dietary uptake of essential

nutritional components such as EPA and DHA (Golden et al., 2021), the ability of the ocean to support this demand under climate change creates a major concern (Colombo et al., 2020). Based on predicted direct temperature effects, Colombo et al. (2020) concluded that, by 2100, the globally available amount of DHA may be reduced by 10%–58% depending on the climate scenario and location.

However, these calculations do not consider ongoing changes within the phytoplankton community structure and its implications for microalgal EPA and DHA content. 'Taxonomic group' has been identified as the major factor accounting for most of the variations in microalgal FA profiles beyond environmental conditions (Galloway & Winder, 2015), with cyanobacteria lacking EPA and DHA altogether (Galloway & Winder, 2015; Jónasdóttir, 2019, this study). It is exactly those cyanobacteria that expand their spatial distribution and dominance under climate change (Flombaum et al., 2013; Paerl & Paul, 2012). The relevance becomes clear in the European shelf regions where rising temperatures and summer droughts enhance thermal stratification and nutrient shortage, which gives a competitive advantage to the picocyanobacterium *Synechococcus* spp. and contributed to a ~50% reduction in summer copepod abundance over the last 60 years (Schmidt et al., 2020). Such changes in the primary producer community can cause a restructuring of intermediate trophic levels and lead to reduced nutritional quality for fish (Heneghan et al., 2023).

In addition to potential roles of temperature and microalgal taxonomy, our Arctic study highlights the importance of nutrient and light availability for marine EPA and DHA inventories. In sea ice of the eutrophic Bering Sea, EPA proportions were four-fold higher for a given presence of EPA-producing diatoms than in sea ice of the oligotrophic CAO. In cultured algae, both taxonomy and changes in the nutrient-light regime caused 3 to 4-fold differences in EPA proportions, despite constant temperatures. These results are in line with previous observations of light- and nutrient-dependent EPA proportions in Arctic field studies (Leu et al., 2010; Nielsen et al., 2023) and experiments with cultured algae (Galloway & Winder, 2015; Guschina & Harwood, 2009; Wacker et al., 2016).

To advance the predictions of marine EPA, DHA production, we suggest, first, to compile available datasets of algal EPA and DHA proportions across large marine ecosystems such as the Arctic to produce a 'present-day reference', and, second, to examine those datasets for the main drivers of EPA and DHA variations in space and time. It is fundamental to separate the two pathways that climate change can affect EPA and DHA proportions of primary producers at ecosystem level: either via taxonomical shifts in the community structure or via increased/decreased proportions within individual species. Direct effects of temperature rise, including the potential to acclimate and adapt (Bishop et al., 2022; O'Donnell et al., 2019) need to be differentiated from indirect effects that modulate light and nutrient regimes via stratification. Future field studies should sample not only for FA proportions, but also estimate their absolute amounts and production, which will further refine our understanding of trophic transfer (Peltomaa et al., 2017). A mechanistic understanding of the key drivers of algal EPA and DHA will improve our projections of the future availability of these highly important biomolecules.

## AUTHOR CONTRIBUTIONS

**Katrin Schmidt:** Conceptualization; data curation; formal analysis; funding acquisition; investigation; methodology; validation; writing – original draft. **Martin Graeve:** Conceptualization; data curation; formal analysis; funding acquisition; methodology; resources; validation; writing – review and editing. **Clara J. M. Hoppe:** Conceptualization; funding acquisition; methodology; validation; writing – review and editing. **Sinhué Torres-Valdes:** Data curation; formal analysis; funding acquisition; methodology; validation; writing – review and editing. **Nahid Welteke:** Formal analysis; methodology; validation; writing – review and editing. **Laura M. Whitmore:** Data curation; funding acquisition; validation; writing – review and editing. **Philipp Anhaus:** Data curation; formal analysis; funding acquisition; methodology; validation; writing – review and editing. **Angus Atkinson:** Funding acquisition; project administration; writing – review and editing. **Simon T. Belt:** Funding acquisition; project administration; resources; writing – review and editing. **Tina Brenneis:** Formal analysis; writing – review and editing. **Robert G. Campbell:** Formal analysis; writing – review and editing. **Giulia Castellani:** Formal analysis; methodology. **Louise A. Copeman:** Data curation; formal analysis; writing – review and editing. **Hauke Flores:** Funding acquisition; resources; writing – review and editing. **Allison A. Fong:** Conceptualization; data curation; funding acquisition; writing – review and editing. **Nicole Hildebrandt:** Formal analysis. **Doreen Kohlbach:** Data curation; formal analysis; methodology; validation; writing – review and editing. **Jens M. Nielsen:** Data curation; formal analysis; methodology; validation; writing – review and editing. **Christopher C. Parrish:** Formal analysis; methodology; validation; writing – review and editing. **Cecilia Rad-Menéndez:** Resources; writing – review and editing. **Sebastian D. Rokitta:** Conceptualization; methodology; resources; writing – review and editing. **Sandra Tippenhauer:** Data curation; resources; validation; writing – review and editing. **Yanpei Zhuang:** Formal analysis; funding acquisition; methodology; validation; writing – review and editing.

## CONFLICT OF INTEREST STATEMENT

The authors declare no conflicts of interest.

## DATA AVAILABILITY STATEMENT

The data that support the findings of this study are openly available in PANGAEA https://www.pangaea.de/ and the UK Polar Data Centre https://www.bas.ac.uk/data/uk-pdc: https://doi.org/10.1594/PANGAEA.935688 (PAR), https://doi.org/10.1594/PANGAEA.959830 (second-year sea ice), https://doi.org/10.1594/PANGAEA.956732 (first-year sea ice), https://doi.pangaea.de/10.1594/PANGAEA.962597 (underway Chl *a*), https://doi.org/10.1594/PANGAEA.959965 (Polarstern-CTD), https://doi.org/10.1594/PANGAEA.959966 (Ocean City-CTD), https://doi.org/10.5285/D7708D08-4BD4-439A-99E2-307A175977EA (fatty acids), https://doi.org/10.5285/bb4b1e74-d5af-4a73-9174-62a01807c641 (cultured algae).

## ORCID

*Katrin Schmidt* https://orcid.org/0000-0002-6488-623X
*Martin Graeve* https://orcid.org/0000-0002-2294-1915
*Clara J. M. Hoppe* https://orcid.org/0000-0002-2509-0546
*Sinhué Torres-Valdes* https://orcid.org/0000-0003-2749-4170
*Nahid Welteke* https://orcid.org/0009-0009-7722-4882
*Laura M. Whitmore* https://orcid.org/0000-0002-2363-4650
*Philipp Anhaus* https://orcid.org/0000-0002-0671-8545
*Angus Atkinson* https://orcid.org/0000-0002-5931-4325
*Simon T. Belt* https://orcid.org/0000-0002-1570-2924
*Tina Brenneis* https://orcid.org/0009-0008-6270-4712
*Robert G. Campbell* https://orcid.org/0000-0002-3710-9750
*Giulia Castellani* https://orcid.org/0000-0001-6151-015X
*Louise A. Copeman* https://orcid.org/0000-0002-8851-7586
*Hauke Flores* https://orcid.org/0000-0003-1617-5449
*Allison A. Fong* https://orcid.org/0000-0002-3779-9624
*Nicole Hildebrandt* https://orcid.org/0000-0003-0555-3096
*Doreen Kohlbach* https://orcid.org/0000-0002-9245-2500
*Jens M. Nielsen* https://orcid.org/0000-0003-3393-4777
*Christopher C. Parrish* https://orcid.org/0000-0002-2386-9556
*Cecilia Rad-Menéndez* https://orcid.org/0000-0001-5248-0948
*Sebastian D. Rokitta* https://orcid.org/0000-0002-7540-9033
*Sandra Tippenhauer* https://orcid.org/0000-0003-3405-6275
*Yanpei Zhuang* https://orcid.org/0000-0002-1409-5640

## REFERENCES

Alonso, D. L., Belarbi, E. H., Fernández-Sevilla, J. M., Rodríguez-Ruiz, J., & Grima, E. M. (2000). Acyl lipid composition variation related to culture age and nitrogen concentration in continuous culture of the microalga *Phaeodactylum tricornutum*. *Phytochemistry*, *54*(5), 461–471.

Aminot, A., Kérouel, R., & Coverly, S. C. (2009). Nutrients in seawater using segmented flow analysis. In O. Wurl (Ed.), *Practical guidelines for the analysis of seawater* (pp. 155–190). CRC Press.

Anderson, B. M., & Ma, D. W. (2009). Are all n-3 polyunsaturated fatty acids created equal? *Lipids in Health and Disease*, *8*(1), 1–20. https://doi.org/10.1186/1476-511X-8-33

Ardyna, M., & Arrigo, K. R. (2020). Phytoplankton dynamics in a changing Arctic Ocean. *Nature Climate Change*, *10*(10), 892–903. https://doi.org/10.1038/s41558-020-0905-y

Ardyna, M., Babin, M., Devred, E., Forest, A., Gosselin, M., Raimbault, P., & Tremblay, J. É. (2017). Shelf-basin gradients shape ecological phytoplankton niches and community composition in the coastal Arctic Ocean (Beaufort Sea). *Limnology and Oceanography*, *62*(5), 2113–2132. https://doi.org/10.1002/lno.10554

Ardyna, M., Babin, M., Gosselin, M., Devred, E., Bélanger, S., Matsuoka, A., & Tremblay, J. É. (2013). Parameterization of vertical chlorophyll a in the Arctic Ocean: Impact of the subsurface chlorophyll maximum on regional, seasonal, and annual primary production estimates. *Biogeosciences*, *10*(6), 4383–4404. https://doi.org/10.5194/bg-10-4383-2013

Ardyna, M., Babin, M., Gosselin, M., Devred, E., Rainville, L., & Tremblay, J. É. (2014). Recent Arctic Ocean sea ice loss triggers novel fall phytoplankton blooms. *Geophysical Research Letters*, *41*(17), 6207–6212. https://doi.org/10.1002/2014GL061047

Ardyna, M., Mundy, C. J., Mayot, N., Matthes, L. C., Oziel, L., Horvat, C., Leu, E., Assmy, P., Hill, V., Matrai, P., Gale, M., Melnikov, I., & Arrigo, K. R. (2020). Under-ice phytoplankton blooms: Shedding light on the "invisible" part of Arctic primary production. *Frontiers in Marine Science*, *7*, 608032. https://doi.org/10.3389/fmars.2020.608032

Ardyna, M., Mundy, C. J., Mills, M. M., Oziel, L., Grondin, P. L., Lacour, L., Verin, G., van Dijken, G., Ras, J., Alou-Font, E., Babin, M., Gosselin, M., Tremblay, J.-É., Raimbault, P., Assmy, P., Nicolaus, M., Claustre, H., & Arrigo, K. R. (2020). Environmental drivers of under-ice phytoplankton bloom dynamics in the Arctic Ocean. *Elementa: Science of the Anthropocene*, *8*, 430. https://doi.org/10.1525/elementa.430

Arrigo, K. R. (2017). Sea ice as a habitat for primary producers. In D. N. Thomas (Ed.), *Sea ice* (pp. 352–369). Wiley-Blackwell.

Assmy, P., Fernández-Méndez, M., Duarte, P., Meyer, A., Randelhoff, A., Mundy, C. J., Olsen, L. M., Kauko, H. M., Bailey, A., Chierici, M., Cohen, L., Doulgeris, A. P., Ehn, J. K., Fransson, A., Gerland, S., Hop, H., Hudson, S. R., Hughes, N., Itkin, P., … Granskog, M. A. (2017). Leads in Arctic pack ice enable early phytoplankton blooms below snow-covered sea ice. *Scientific Reports*, *7*(1), 40850. https://doi.org/10.1038/srep40850

Baird, P. (2022). Diatoms and fatty acid production in Arctic and estuarine ecosystems a reassessment of marine food webs, with a focus on the timing of shorebird migration. *Marine Ecology*

*Progress Series*, *688*, 173–196. https://doi.org/10.3354/meps14025

Bishop, I. W., Anderson, S. I., Collins, S., & Rynearson, T. A. (2022). Thermal trait variation may buffer Southern Ocean phytoplankton from anthropogenic warming. *Global Change Biology*, *28*(19), 5755–5767.

Budge, S. M., Wooller, M. J., Springer, A. M., Iverson, S. J., McRoy, C. P., & Divoky, G. J. (2008). Tracing carbon flow in an arctic marine food web using fatty acid-stable isotope analysis. *Oecologia*, *157*, 117–129. https://doi.org/10.1007/s00442-008-1053-7

Calder, P. C. (2015). Functional roles of fatty acids and their effects on human health. *Journal of Parenteral and Enteral Nutrition*, *39*, 18S–32S. https://doi.org/10.1177/0148607115595980

Campbell, K., Mundy, C. J., Juhl, A. R., Dalman, L. A., Michel, C., Galley, R. J., Else, B. E., Geilfus, N. X., & Rysgaard, S. (2019). Melt procedure affects the photosynthetic response of sea ice algae. *Frontiers in Earth Science*, *7*, 21. https://doi.org/10.3389/feart.2019.00021

Castellani, G., Veyssière, G., Karcher, M., Stroeve, J., Banas, S. N., Bouman, A. H., Brierley, S. A., Connan, S., Cottier, F., Große, F., Hobbs, L., Katlein, C., Light, B., Mckee, D., Orkney, A., Proud, R., & Schourup-Kristensen, V. (2022). Shine a light: Under-ice light and its ecological implications in a changing Arctic Ocean. *Ambio*, *51*, 307–317. https://doi.org/10.1007/s13280-021-01662-3

Clegg, M. R., Maberly, S. C., & Jones, R. I. (2003). The effect of photon irradiance on the behavioral ecology and potential niche separation of freshwater phytoplanktonic flagellates. *Journal of Phycology*, *39*(4), 650–662. https://doi.org/10.1046/j.1529-8817.2003.02164.x

Colombo, S. M., Rodgers, T. F., Diamond, M. L., Bazinet, R. P., & Arts, M. T. (2020). Projected declines in global DHA availability for human consumption as a result of global warming. *Ambio*, *49*(4), 865–880. https://doi.org/10.1007/s13280-019-01234-6

Colombo, S. M., Wacker, A., Parrish, C. C., Kainz, M. J., & Arts, M. T. (2017). A fundamental dichotomy in long-chain polyunsaturated fatty acid abundance between and within marine and terrestrial ecosystems. *Environmental Reviews*, *25*(2), 163–174. https://doi.org/10.1139/er-2016-0062

Dalsgaard, J., John, M. S., Kattner, G., Müller-Navarra, D., & Hagen, W. (2003). Fatty acid trophic markers in the pelagic marine environment. *Advances in Marine Biology*, *46*, 225–340. https://doi.org/10.1016/s0065-2881(03)46005-7

DeLong, E. F., & Yayanos, A. A. (1985). Adaptation of the membrane lipids of a deep-sea bacterium to changes in hydrostatic pressure. *Science*, *228*(4703), 1101–1103.

Duerksen, S. W., Thiemann, G. W., Budge, S. M., Poulin, M., Niemi, A., & Michel, C. (2014). Large, omega-3 rich, pelagic diatoms under Arctic sea ice: Sources and implications for food webs. *PLoS One*, *9*(12), e114070.

Falkowski, P. G., & Owens, T. G. (1980). Light-shade adaptation – 2 strategies in marine-phytoplankton. *Plant Physiology*, *66*, 592–595. https://doi.org/10.1104/pp.66.4.592

Fernández-Méndez, M., Wenzhöfer, F., Peeken, I., Sørensen, H. L., Glud, R. N., & Boetius, A. (2014). Composition, buoyancy regulation and fate of ice algal aggregates in the Central Arctic Ocean. *PLoS One*, *9*(9), e107452. https://doi.org/10.1371/journal.pone.0107452

Flombaum, P., Gallegos, J. L., Gordillo, R. A., Rincón, J., Zabala, L. L., Jiao, N., Karl, D. M., Li, W. K., Lomas, M. W., Veneziano, D., Vera, C. S., Vrugt, J. A., & Martiny, A. C. (2013). Present and future global distributions of the marine Cyanobacteria *Prochlorococcus* and *Synechococcus*. *Proceedings of the National Academy of Sciences of the United States of America*, *110*(24), 9824–9829.

Flores, H., David, C., Ehrlich, J., Hardge, K., Kohlbach, D., Lange, B. A., Niehoff, B., Nöthig, E. M., Peeken, I., & Metfies, K. (2019). Sea-ice properties and nutrient concentration as drivers of the taxonomic and trophic structure of high-Arctic protist and metazoan communities. *Polar Biology*, *42*, 1377–1395. https://doi.org/10.1007/s00300-019-02526-z

Flores, H., Veyssière, G., Castellani, G., Wilkinson, J., Hoppmann, M., Karcher, M., Valcic, L., Cornils, A., Geoffroy, M., Nicolaus, M., & Stroeve, J. (2023). Sea-ice decline could keep zooplankton deeper for longer. *Nature Climate Change*, *13*, 1122–1130.

Frey, K. E., Comiso, J. C., Cooper, L. W., Garcia-Eidell, C., Grebmeier, J. M., & Stock, L. V. (2022). Arctic ocean primary productivity: The response of marine algae to climate warming and sea ice decline. *Arctic Report Card*.

Fuschino, J. R., Guschina, I. A., Dobson, G., Yan, N. D., Harwood, J. L., & Arts, M. T. (2011). Rising water temperatures alter lipid dynamics and reduce n-3 essential fatty acid concentrations in *Scenedesmus obliquus* (Chlorophyta). *Journal of Phycology*, *47*(4), 763–774.

Galloway, A. W., Britton-Simmons, K. H., Duggins, D. O., Gabrielson, P. W., & Brett, M. T. (2012). Fatty acid signatures differentiate marine macrophytes at ordinal and family ranks. *Journal of Phycology*, *48*(4), 956–965.

Galloway, A. W., & Winder, M. (2015). Partitioning the relative importance of phylogeny and environmental conditions on phytoplankton fatty acids. *PLoS One*, *10*(6), e0130053.

Garrison, D. L., & Buck, K. R. (1986). Organism losses during ice melting: A serious bias in sea ice community studies. *Polar Biology*, *6*, 237–239.

Gladyshev, M. I., Arts, M. T., & Sushchik, N. I. (2009). Preliminary estimates of the export of omega-3 highly unsaturated fatty acids (EPA + DHA) from aquatic to terrestrial ecosystems. In M. T. Brett, M. T. Arts, & M. J. Kainz (Eds.), *Lipids in aquatic ecosystems* (pp. 179–210). Springer.

Golden, C. D., Koehn, J. Z., Shepon, A., Passarelli, S., Free, C. M., Viana, D. F., Matthey, H., Eurich, J. G., Gephart, J. A., Fluet-Chouinard, E., Nyboer, E. A., Lynch, A. J., Kjellevold, M., Bromage, S., Charlebois, P., Barange, M., Vannuccini, S., Cao, L., Kleisner, K. M., ... Thilsted, S. H. (2021). Aquatic foods to nourish nations. *Nature*, *598*(7880), 315–320.

Graeve, M., Kattner, G., Wiencke, C., & Karsten, U. (2002). Fatty acid composition of Arctic and Antarctic macroalgae: Indicator of phylogenetic and trophic relationships. *Marine Ecology Progress Series*, *231*, 67–74.

Grasshoff, K., Kremling, K., & Ehrhardt, M. (Eds.). (2009). *Methods of seawater analysis*. John Wiley & Sons.

Guillard, R. R. L., & Ryther, J. H. (1962). Studies of marine planktonic diatoms. I. *Cyclotella nana* Hustedt and *Detonula confervacea* Cleve. *Canadian Journal of Microbiology*, *8*, 229–239.

Guschina, I. A., & Harwood, J. L. (2009). Algal lipids and effect of the environment on their biochemistry. In M. T. Arts, M. T. Brett, & M. Kainz (Eds.), *Lipids in aquatic ecosystems* (pp. 1–24). Springer.

Hamilton, M. L., Warwick, J., Terry, A., Allen, M. J., Napier, J. A., & Sayanova, O. (2015). Towards the industrial production of omega-3 long chain polyunsaturated fatty acids from a genetically modified diatom *Phaeodactylum tricornutum*. *PLoS One*, *10*(12), e0144054.

Heneghan, R. F., Everett, J. D., Blanchard, J. L., Sykes, P., & Richardson, A. J. (2023). Climate-driven zooplankton shifts cause large-scale declines in food quality for fish. *Nature Climate Change*, *13*, 470–477. https://doi.org/10.1038/s41558-023-01630-7

Hixson, S. M., & Arts, M. T. (2016). Climate warming is predicted to reduce omega-3, long-chain, polyunsaturated fatty acid production in phytoplankton. *Global Change Biology*, *22*(8), 2744–2755.

Hobbs, L., Banas, N. S., Cottier, F. R., Berge, J., & Daase, M. (2020). Eat or sleep: Availability of winter prey explains mid-winter and spring activity in an Arctic *Calanus* population. *Frontiers in Marine Science*, *7*, 541564. https://doi.org/10.3389/fmars.2020.541564

Jónasdóttir, S. H. (2019). Fatty acid profiles and production in marine phytoplankton. *Marine Drugs*, *17*(3), 151.

Jónasdóttir, S. H., Fields, D., & Pantoja, S. (1995). Copepod egg production in Long Island Sound, USA, as a function of the chemical composition of seston. *Marine Ecology Progress Series*, *119*(1), 87–98.

Juranek, L. W. (2022). Changing biogeochemistry of the Arctic Ocean. *Oceanography*, *35*(3/4), 144–155.

Kainz, M., Arts, M. T., & Mazumder, A. (2004). Essential fatty acids in the planktonic food web and their ecological role for higher trophic levels. *Limnology and Oceanography*, *49*(5), 1784–1793.

Katlein, C., Schiller, M., Belter, H. J., Coppolaro, V., Wenslandt, D., & Nicolaus, M. (2017). A new remotely operated sensor platform for interdisciplinary observations under sea ice. *Frontiers in Marine Science*, *4*, 281. https://doi.org/10.3389/fmars.2017.00281

Kattner, G., & Fricke, H. S. (1986). Simple gas-liquid chromatographic method for the simultaneous determination of fatty acids and alcohols in wax esters of marine organisms. *Journal of Chromatography A*, *361*, 263–268.

Kipp, L. E., Charette, M. A., Moore, W. S., Henderson, P. B., & Rigor, I. G. (2018). Increased fluxes of shelf-derived materials to the Central Arctic Ocean. *Science Advances*, *4*(1), eaao1302.

Kirkwood, D. (1996). *Nutrients: Practical notes on their determination in sea water*. International Council for the Exploration of the Sea.

Knap, A., Michaels, A., Close, A., Ducklow, H., & Dickson, A. (1996). *Protocols for the Joint Global Ocean Flux Study (JGOFS) core measurements*. JGOFS Report No. 19, Reprint of the IOC Manuals and Guides No. 29, UNESCO, Paris, pp. 43–90.

Knust, R. (2017). Polar research and supply vessel POLARSTERN operated by the Alfred-Wegener-Institute. *Journal of Large-Scale Research Facilities JLSRF*, *3*, A119.

Kohlbach, D., Duerksen, S. W., Lange, B. A., Charette, J., Reppchen, A., Tremblay, P., Campbell, K. L., Ferguson, S. H., & Michel, C. (2020). Fatty acids and stable isotope signatures of first-year and multi-year sea ice in the Canadian High Arctic. *Elementa: Science of the Anthropocene*, *8*(1), 054.

Kohlbach, D., Graeve, M., Lange, A., David, C., Peeken, I., & Flores, H. (2016). The importance of ice algae-produced carbon in the Central Arctic Ocean ecosystem: Food web relationships revealed by lipid and stable isotope analyses. *Limnology and Oceanography*, *61*(6), 2027–2044. https://doi.org/10.1002/lno.10351

Kohlbach, D., Hop, H., Wold, A., Schmidt, K., Smik, L., Belt, S. T., Keck Al-Habahbeh, A., Woll, M., Graeve, M., Dąbrowska, A. M., Tatarek, A., Atkinson, A., & Assmy, P. (2021). Multiple trophic markers trace dietary carbon sources in Barents Sea zooplankton during late summer. *Frontiers in Marine Science*, *7*, 610248.

Kohlbach, D., Smik, L., Belt, S. T., Hop, H., Wold, A., Graeve, M., & Assmy, P. (2022). A multi-trophic marker approach reveals high feeding plasticity in Barents Sea under-ice fauna. *Progress in Oceanography*, *208*, 102895.

Krause, J. W., Schulz, I. K., Rowe, K. A., Dobbins, W., Winding, M. H., Sejr, M. K., Duarte, C. M., & Agustí, S. (2019). Silicic acid limitation drives bloom termination and potential carbon sequestration in an Arctic bloom. *Scientific Reports*, *9*(1), 8149.

Krumpen, T., Birrien, F., Kauker, F., Rackow, T., von Albedyll, L., Angelopoulos, M., Belter, H. J., Bessonov, V., Damm, E., Dethloff, K., Haapala, J., Haas, C., Harris, C., Hendricks, S., Hoelemann, J., Hoppmann, M., Kaleschke, L., Karcher, M., Kolabutin, N., … Watkins, D. (2020). The MOSAiC ice floe: Sediment-laden survivor from the Siberian shelf. *The Cryosphere*, *14*(7), 2173–2187.

Laukert, G., Grasse, P., Novikhin, A., Povazhnyi, V., Doering, K., Hölemann, J., Janout, M., Bauch, D., Kassens, H., & Frank, M. (2022). Nutrient and silicon isotope dynamics in the Laptev Sea and implications for nutrient availability in the transpolar drift. *Global Biogeochemical Cycles*, *36*(9), e2022GB007316.

Leu, E., Brown, T. A., Graeve, M., Wiktor, J., Hoppe, C. J., Chierici, M., Fransson, A., Verbiest, S., Kvernvik, A. C., & Greenacre, M. J. (2020). Spatial and temporal variability of ice algal trophic markers—With recommendations about their application. *Journal of Marine Science and Engineering*, *8*(9), 676.

Leu, E., Falk-Petersen, S., Kwaśniewski, S., Wulff, A., Edvardsen, K., & Hessen, D. O. (2006). Fatty acid dynamics during the spring bloom in a High Arctic fjord: Importance of abiotic factors versus community changes. *Canadian Journal of Fisheries and Aquatic Sciences*, *63*(12), 2760–2779.

Leu, E., Wiktor, J., Søreide, J. E., Berge, J., & Falk-Petersen, S. (2010). Increased irradiance reduces food quality of sea ice algae. *Marine Ecology Progress Series*, *411*, 49–60.

Lewis, K. M., Van Dijken, G. L., & Arrigo, K. R. (2020). Changes in phytoplankton concentration now drive increased Arctic Ocean primary production. *Science*, *369*(6500), 198–202. https://doi.org/10.1126/science.aay8380

Li, W. K., McLaughlin, F. A., Lovejoy, C., & Carmack, E. C. (2009). Smallest algae thrive as the Arctic Ocean freshens. *Science*, *326*(5952), 539. https://doi.org/10.1126/science.1179798

Litzow, M. A., Bailey, K. M., Prahl, F. G., & Heintz, R. (2006). Climate regime shifts and reorganization of fish communities: The essential fatty acid limitation hypothesis. *Marine Ecology Progress Series*, *315*, 1–11.

Lynn, S. G., Kilham, S. S., Kreeger, D. A., & Interlandi, S. J. (2000). Effect of nutrient availability on the biochemical and elemental stoichiometry in the freshwater diatom *Stephanodiscus minutulus* (Bacillariophyceae). *Journal of Phycology*, *36*(3), 510–522.

Marmillot, V., Parrish, C. C., Tremblay, J. É., Gosselin, M., & MacKinnon, J. F. (2020). Environmental and biological determinants of algal lipids in Western Arctic and subarctic seas. *Frontiers in Environmental Science*, *8*, 538635.

Matrai, P. A., Olson, E., Suttles, S., Hill, V., Codispoti, L. A., Light, B., & Steele, M. (2013). Synthesis of primary production in the Arctic Ocean: I. Surface waters, 1954–2007. *Progress in Oceanography*, *110*, 93–106.

Mock, T., & Kroon, B. M. (2002). Photosynthetic energy conversion under extreme conditions—II: The significance of lipids under light limited growth in Antarctic sea ice diatoms. *Phytochemistry*, *61*(1), 53–60.

Nicolaus, M., Hudson, S. R., Gerland, S., & Munderloh, K. (2010). A modern concept for autonomous and continuous measurements of spectral albedo and transmittance of sea ice. *Cold Regions Science and Technology*, *62*(1), 14–28.

Nicolaus, M., Perovich, D. K., Spreen, G., Granskog, M. A., von Albedyll, L., Angelopoulos, M., Philipp, A., Stefanie, A., Jakob, B. H., Vladimir, B., Gerit, B., Jörg, B., Radiance, C., Estel, C., Bin, C., David, C.-S., Ruzica, D., Ellen, D., Gijs, D. B., … Wendisch, M. (2022). Overview of the MOSAiC expedition: Snow and sea ice. *Elementa: Science of the Anthropocene*, *10*(1), 000046.

Nielsen, J. M., Copeman, L. A., Eisner, L. B., Axler, K. E., Mordy, C. W., & Lomas, M. W. (2023). Phytoplankton and seston fatty acid dynamics in the northern Bering-Chukchi Sea region. *Deep Sea Research Part II: Topical Studies in Oceanography*, *208*, 105247.

Nixdorf, U., Dethloff, K., Rex, M., Shupe, M., Sommerfeld, A., Perovich, D. K., Marcel, N., Céline, H., Benjamin, R., Brice, L., Ellen, D., Rolf, G., Allison, F., Wieslaw, M., Annette, R., Ronald, K., Gunnar, S., Manfred, W., Andreas, H., & Boetius, A. (2021). *MOSAiC extended acknowledgement*. Zenodo. https://doi.org/10.5281/zenodo.5541624

O'Donnell, D. R., Du, Z. Y., & Litchman, E. (2019). Experimental evolution of phytoplankton fatty acid thermal reaction norms. *Evolutionary Applications*, *12*(6), 1201–1211.

Orkney, A., Platt, T., Narayanaswamy, B. E., Kostakis, I., & Bouman, H. A. (2020). Bio-optical evidence for increasing *Phaeocystis* dominance in the Barents Sea. *Philosophical Transactions of the Royal Society A*, *378*(2181), 20190357.

Oziel, L., Baudena, A., Ardyna, M., Massicotte, P., Randelhoff, A., Sallée, J. B., Ingvaldsen, R. B., Devred, E., & Babin, M. (2020). Faster Atlantic currents drive poleward expansion of temperate phytoplankton in the Arctic Ocean. *Nature Communications*, *11*, 1705. https://doi.org/10.1038/s41467-020-15485-5

Oziel, L., Neukermans, G., Ardyna, M., Lancelot, C., Tison, J. L., Wassmann, P., Sirven, J., Ruiz-Pino, D., & Gascard, J. C. (2017).

Role for Atlantic inflows and sea ice loss on shifting phytoplankton blooms in the Barents Sea. *Journal of Geophysical Research: Oceans*, *122*(6), 5121–5139.

Paerl, H. W., & Paul, V. J. (2012). Climate change: Links to global expansion of harmful cyanobacteria. *Water Research*, *46*(5), 1349–1363.

PAME. (2014). *Large marine ecosystems.* https://www.pame.is/projects/ecosystem-approach/arctic-large-marine-ecosystems-lme-s

Parrish, C. C. (2009). Essential fatty acids in aquatic food webs. In M. Kainz, M. T. Brett, & M. T. Arts (Eds.), *Lipids in aquatic ecosystems* (pp. 309–326). Springer.

Parrish, C. C. (2013). Lipids in marine ecosystems. *International Scholarly Research Notices*, *2013*, 604045.

Parzanini, C., Parrish, C. C., Hamel, J. F., & Mercier, A. (2019). Reviews and syntheses: Insights into deep-sea food webs and global environmental gradients revealed by stable isotope ($\delta^{15}$N, $\delta^{13}$C) and fatty acid trophic biomarkers. *Biogeosciences*, *16*(14), 2837–2856.

Paulsen, M. L., Doré, H., Garczarek, L., Seuthe, L., Müller, O., Sandaa, R.-A., Bratbak, G., & Larsen, A. (2016). *Synechococcus* in the Atlantic gateway to the Arctic Ocean. *Frontiers in Marine Science*, *3*, 191. https://doi.org/10.3389/fmars.2016.00191

Peltomaa, E., Johnson, M. D., & Taipale, S. J. (2017). Marine cryptophytes are great sources of EPA and DHA. *Marine Drugs*, *16*(1), 3.

Pond, D. W., & Harris, R. P. (1996). The lipid composition of the coccolithophore *Emiliania huxleyi* and its possible ecophysiological significance. *Journal of the Marine Biological Association of the United Kingdom*, *76*(3), 579–594.

Rabe, B., Heuzé, C., Regnery, J., Aksenov, Y., Allerholt, J., Athanase, M., Bai, Y., Basque, C., Bauch, D., Baumann, T. M., Chen, D., Cole, S. T., Craw, L., Davies, A., Damm, E., Dethloff, K., Divine, D. V., Doglionli, F., Ebert, F., … Zhu, J. (2022). Overview of the MOSAiC expedition: Physical oceanography. *Elementa: Science of the Anthropocene*, *10*(1), 62. https://doi.org/10.1525/elementa.2021.00062

Randelhoff, A., Holding, J., Janout, M., Sejr, M. K., Babin, M., Tremblay, J. É., & Alkire, M. B. (2020). Pan-Arctic Ocean primary production constrained by turbulent nitrate fluxes. *Frontiers in Marine Science*, *7*, 150. https://doi.org/10.3389/fmars.2020.00150

Raven, J. A., Kübler, J. E., & Beardall, J. (2000). Put out the light, and then put out the light. *Journal of the Marine Biological Association of the United Kingdom*, *80*(1), 1–25. https://doi.org/10.1017/S0025315499001526

Reuss, N., & Poulsen, L. (2002). Evaluation of fatty acids as biomarkers for a natural plankton community. A field study of a spring bloom and a post-bloom period off West Greenland. *Marine Biology*, *141*, 423–434. https://doi.org/10.1007/s00227-002-0841-6

Rimm, E. B., Appel, L. J., Chiuve, S. E., Djoussé, L., Engler, M. B., Kris-Etherton, P. M., Mozaffarian, D., Siscovick, D. S., & Lichtenstein, A. H. (2018). Seafood long-chain n-3 polyunsaturated fatty acids and cardiovascular disease: A science advisory from the American Heart Association. *Circulation*, *138*(1), e35–e47. https://doi.org/10.1161/CIR.0000000000000574

Rousch, J. M., Bingham, S. E., & Sommerfeld, M. R. (2003). Changes in fatty acid profiles of thermo-intolerant and thermo-tolerant marine diatoms during temperature stress. *Journal of Experimental Marine Biology and Ecology*, *295*(2), 145–156. https://doi.org/10.1016/S0022-0981(03)00293-4

Sakinan, S., Lawson, G. L., Wiebe, P. H., Chu, D., & Copley, N. J. (2019). Accounting for seasonal and composition-related variability in acoustic material properties in estimating copepod and krill target strength. *Limnology and Oceanography: Methods*, *17*(11), 607–625. https://doi.org/10.1002/lom3.10336

Schmidt, K., Atkinson, A., Venables, H. J., & Pond, D. W. (2012). Early spawning of Antarctic krill in the Scotia Sea is fuelled by "superfluous" feeding on non-ice associated phytoplankton blooms. *Deep Sea Research Part II: Topical Studies in Oceanography*, *59*, 159–172. https://doi.org/10.1016/j.dsr2.2011.05.002

Schmidt, K., Birchill, A. J., Atkinson, A., Brewin, R. J., Clark, J. R., Hickman, A. E., Johns, D. G., Lohan, M. C., Milne, A., Pardo, S., Polimene, L., Smyth, T. J., Tarran, G. A., Widdicombe, C. E., Woodward, E. M. S., & Ussher, S. J. (2020). Increasing picocyanobacteria success in shelf waters contributes to long-term food web degradation. *Global Change Biology*, *26*(10), 5574–5587. https://doi.org/10.1111/gcb.15161

Shupe, M. D., Rex, M., Blomquist, B., Persson, P. O. G., Schmale, J., Uttal, T., Althausen, D., Angot, H., Archer, S., Bariteau, L., Beck, I., Bilberry, J., Boyer, M., Brasseur, Z., Brooks, I. M., Bucci, S., Buck, C., Calmer, R., Cassano, J., … Yue, F. (2022). Overview of the MOSAiC expedition: Atmosphere. *Elementa: Science of the Anthropocene*, *10*(1), 60. https://doi.org/10.1525/elementa.2021.00060

Sinensky, M. (1974). Homeoviscous adaptation—A homeostatic process that regulates the viscosity of membrane lipids in *Escherichia coli*. *Proceedings of the National Academy of Sciences of the United States of America*, *71*(2), 522–525. https://doi.org/10.1073/pnas.71.2.522

Søreide, J. E., Leu, E. V., Berge, J., Graeve, M., & Falk-Petersen, S. T. I. G. (2010). Timing of blooms, algal food quality and *Calanus glacialis* reproduction and growth in a changing Arctic. *Global Change Biology*, *16*(11), 3154–3163. https://doi.org/10.1111/j.1365-2486.2010.02175.x

Spilling, K., & Markager, S. (2008). Ecophysiological growth characteristics and modeling of the onset of the spring bloom in the Baltic Sea. *Journal of Marine Systems*, *73*(3–4), 323–337. https://doi.org/10.1016/j.jmarsys.2006.10.012

Terhaar, J., Lauerwald, R., Regnier, P., Gruber, N., & Bopp, L. (2021). Around one third of current Arctic Ocean primary production sustained by rivers and coastal erosion. *Nature Communications*, *12*(1), 169. https://doi.org/10.1038/s41467-020-20470-z

Thompson, G. A., Jr. (1996). Lipids and membrane function in green algae. *Biochimica et Biophysica acta (BBA)-Lipids and Lipid Metabolism*, *1302*(1), 17–45. https://doi.org/10.1016/0005-2760(96)00045-8

Tippenhauer, S., Vredenborg, M., Heuzé, C., Ulfsbo, A., Rabe, B., Granskog, M. A., Allerholt, J., Balmonte, J. P., Campbell, R. G., Castellani, G., Chamberlain, E., Creaman, J., D'Angelo, A., Dietrich, U., Droste, E. S., Eggers, L., Fang, Y.-C., Fong, A. A., Gardner, J., … Zhuang, Y. (2023a). *Physical oceanography water bottle samples based on ship CTD during POLARSTERN cruise PS122* [Data set]. https://doi.org/10.1594/PANGAEA.959965

Tippenhauer, S., Vredenborg, M., Heuzé, C., Ulfsbo, A., Rabe, B., Granskog, M. A., Allerholt, J., Balmonte, J. P., Campbell, R. G., Castellani, G., Chamberlain, E., Creaman, J., D'Angelo, A., Dietrich, U., Droste, E. S., Eggers, L., Fang, Y.-C., Fong, A. A., Gardner, J., … Zhuang, Y. (2023b). *Physical oceanography water bottle samples based on Ocean City CTD during POLARSTERN cruise PS122.* [Dataset]. https://doi.org/10.1594/PANGAEA.959966

Tittensor, D. P., Novaglio, C., Harrison, C. S., Heneghan, R. F., Barrier, N., Bianchi, D., Bopp, L., Bryndum-Buchholz, A., Britten, G. L., Büchner, M., Cheung, W. W. L., Christensen, V., Coll, M., Dunne, J. P., Eddy, T. D., Everett, J. D., Fernandes-Salvador, J. A., Fulton, E. A., Galbraith, E. D., … Blanchard, J. L. (2021). Next-generation ensemble projections reveal higher climate risks for marine ecosystems. *Nature Climate Change*, *11*, 973–981. https://doi.org/10.1038/s41558-021-01173-9

Tremblay, J. É., Bélanger, S., Barber, D. G., Asplin, M., Martin, J., Darnis, G., Fortier, L., Gratton, Y., Link, H., Archambault, P., Sallon, A., Michel, C., Williams, W. J., Philippe, B., & Gosselin, M. (2011). Climate forcing multiplies biological productivity in the coastal Arctic Ocean. *Geophysical Research Letters*, *38*(18), 48825. https://doi.org/10.1029/2011GL048825

Tuerena, R. E., Hopkins, J., Buchanan, P. J., Ganeshram, R. S., Norman, L., von Appen, W. J., Tagliabue, A., Doncila, A., Graeve, M., Ludwichowski, K. U., Dodd, P. A., de la Vega, C., Salter, I., & Mahaffey, C. (2021). An Arctic strait of two halves: The changing

dynamics of nutrient uptake and limitation across the Fram Strait. *Global Biogeochemical Cycles*, *35*(9), e2021GB006961. https://doi.org/10.1029/2021GB006961

Wacker, A., Piepho, M., Harwood, J. L., Guschina, I. A., & Arts, M. T. (2016). Light-induced changes in fatty acid profiles of specific lipid classes in several freshwater phytoplankton species. *Frontiers in Plant Science*, *7*, 264. https://doi.org/10.3389/fpls.2016.00264

Wacker, A., Piepho, M., & Spijkerman, E. (2015). Photosynthetic and fatty acid acclimation of four phytoplankton species in response to light intensity and phosphorus availability. *European Journal of Phycology*, *50*(3), 288–300. https://doi.org/10.1080/09670262.2015.1050068

Wang, S. W., Budge, S. M., Gradinger, R. R., Iken, K., & Wooler, M. J. (2014). Fatty acid and stable isotope characteristics of sea ice and pelagic particulate organic matter in the Bering Sea: Tools for estimating sea ice algal contribution to Arctic food web production. *Oecologia*, *174*(3), 699–712. https://doi.org/10.1007/s00442-013-2832-3

## SUPPORTING INFORMATION

Additional supporting information can be found online in the Supporting Information section at the end of this article.